AFRL-RV-HA-TR-2007-1143

Space Particle Hazard Specification, Forecasting, and Mitigation

James Metcalf
Donald Brautigam
David Cooke
Bronek Dichter
Gregory Ginet
Robert Hilmer
Katharine Kadinsky-Cade
Kevin Ray
Michael Starks
Adrian Wheelock

Final Report

30 November 2007

AIR FORCE RESEARCH LABORATORY
AIR FORCE MATERIEL COMMAND
Space Vehicles Directorate
29 Randolph Rd.
Hanscom AFB, MA 01731-3010

AFRL-RV-HA-TR-2007-1143

This technical report has been reviewed and is approved for publication.

/signed/
Robert A. Morris, Chief
Battlespace Environment Division

/signed/   /signed/
James I. Metcalf   Joel B. Mozer, Chief
Research Physicist   Space Weather Center of Excellence

REPORT DOCUMENTATION PAGE

Form Approved
OMB No. 0704-0188

1. REPORT DATE *(DD-MM-YYYY)* 11-30-2007	2. REPORT TYPE Scientific Report - Final	3. DATES COVERED *(From - To)* 10-01-2001 to 09-30-2007

4. TITLE AND SUBTITLE	5a. CONTRACT NUMBER
Space Particle Hazard Specification, Forecasting, and Mitigation	N/A

5b. GRANT NUMBER
N/A

5c. PROGRAM ELEMENT NUMBER
63401F

6. AUTHOR(S)	5d. PROJECT NUMBER
J. Metcalf, D. Brautigam, D. Cooke, B. Dichter, G. Ginet, R. Hilmer, K. Kadinsky-Cade, K. Ray, M. Starks, & A. Wheelock	5021

5e. TASK NUMBER
5021RS

5f. WORK UNIT NUMBER
5021RSA1

7. PERFORMING ORGANIZATION NAME(S) AND ADDRESS(ES) Air Force Research Laboratory/RVBXR 29 Randolph Rd. Hanscom AFB, MA 01731-3010	8. PERFORMING ORGANIZATION REPORT NUMBER AFRL-RV-HA-TR-2007-1143

9. SPONSORING / MONITORING AGENCY NAME(S) AND ADDRESS(ES) Air Force Research Laboratory/RVBXR 29 Randolph Rd. Hanscom AFB, MA 01731-3010	10. SPONSOR/MONITOR'S ACRONYM(S)

11. SPONSOR/MONITOR'S REPORT NUMBER(S)

12. DISTRIBUTION / AVAILABILITY STATEMENT

Approved for Public Release; Distribution Unlimited.

13. SUPPLEMENTARY NOTES

14. ABSTRACT
This report describes R&D to measure and model the near-Earth space environment and its effects on spacecraft in orbit. A Compact Environmental Anomaly Sensor (CEASE) was developed, and two versions of the instrument were flown in two different orbital domains. Other space environment instruments are being developed for flight on the Demonstration and Science Experiment (DSX) satellite. Data from CEASE and other sensors were used to develop new models of the space environment, which have been incorporated into AF-GEOSpace, a software program that includes many space environment models, applications, and data visualization products. Spacecraft charging technology includes development of the NASA-Air Force Spacecraft Charging Analyzer Program (NASCAP-2K) to model interactions between spacecraft surfaces and plasma environments and a Satellite Charge/Discharge Product (Char/D) to create tailored system-impact decision aids related to both surface and deep charging of satellites. NASCAP-2K has been used in the design of spacecraft components and in the analysis of on-orbit anomalies. We developed a second-generation Charge Control System (CCS-II), which is designed to emit xenon plasma to neutralize electrostatic charge on a spacecraft, and explored alternative charge mitigation techniques.

15. SUBJECT TERMS
Energetic electrons, energetic protons, spacecraft charging

16. SECURITY CLASSIFICATION OF:			17. LIMITATION OF ABSTRACT	18. NUMBER OF PAGES	19a. NAME OF RESPONSIBLE PERSON James Metcalf
a. REPORT UNCLASSIFIED	**b. ABSTRACT** UNCLASSIFIED	**c. THIS PAGE** UNCLASSIFIED	UNL	42	19b. TELEPHONE NUMBER *(include area code)*

Standard Form 298 (Rev. 8-98)
Prescribed by ANSI Std. Z39.18

[Reverse side of SF 298 is blank]

Table of Contents

Figures

1. SUMMARY

This report describes research and development conducted by the Air Force Research Laboratory (AFRL) to measure and model the near-Earth space environment and the effects of the environment on spacecraft in orbit. A Compact Environmental Anomaly Sensor (CEASE) was developed, and two versions of the instrument were flown in two different orbital domains. Other space environment instruments are being developed for flight on the Demonstration and Science Experiment (DSX) satellite, which is expected to be launched in 2010. Data from CEASE and other sensors are being used to develop new models of the space environment, with particular emphasis on the radiation belts. New and improved models of the space environment are incorporated into AF-GEOSpace, a user-friendly, graphics-intensive software program that includes many space environment models, applications, and data visualization products developed by AFRL and others in the space weather community. AF-GEOSpace software has been distributed to over 500 recipients in DoD and other government organizations, national laboratories, spacecraft related industry, and research universities. Work has begun on a new standard model of the radiation belts, which will be included in a future version of AF-GEOSpace.

Research and development on spacecraft charging aims to understand the mechanisms of charging, model the distribution of charge on spacecraft, and develop techniques to mitigate charging and its adverse effects. AFRL scientists collaborate with contractors to develop the NASA-Air Force Spacecraft Charging Analyzer Program (NASCAP-2K). NASCAP-2K is a three-dimensional computer code that models interactions between spacecraft surfaces and plasma environments, including plasmas emitted from spacecraft sources. It has been used in the design of spacecraft components and in the analysis of on-orbit anomalies. We developed Version 1.0 of the Satellite Charge/Discharge Product (Char/D) for the Technology Applications Division of the Space and Missile Systems Center at Peterson Air Force Base, Colo. Char/D combines observations and modeling of a wide range of electron energies in many magnetospheric regions to create tailored system-impact decision aids related to the specification and forecast of both surface and deep charging of satellites. We developed a second-generation Charge Control System (CCS-II), which is designed to emit xenon plasma to neutralize electrostatic charge on a spacecraft. In collaboration with MIT Lincoln Laboratory we began to develop the Ion-Proportional Surface Emission Cathode (IProSEC) as an alternative approach to the mitigation of spacecraft charging.

2. INTRODUCTION

This report describes Advanced Development (R&D Category 6.3) work in the Space Particle Hazard Specification and Forecasting Program. The program comprises three major areas of investigation, described in the following subsections. Space environment instruments are developed, both in-house and on contract. The analysis of data from these and other instruments constitutes one of the main thrusts of the Exploratory Development (R&D Category 6.2) work. New and improved models of the space

environment are developed under 6.2 funding; the incorporation of these models into the AF-GEOSpace suite is supported by 6.3 funding. The interactions of spacecraft with their environment have been investigated both empirically and theoretically, with the goal of quantifying environmental hazards, especially those related to spacecraft charging, and mitigating their impact. The Exploratory Development work of the program is described by Metcalf et al. (2007).

Space particles pose a variety of hazards to satellites. These include, but are not limited to, single event effects on microelectronics (>10 MeV ions), total dose degradation of microelectronics (>10 MeV ions, >0.5 MeV electrons), electrostatic discharge resulting from the differential accumulation of electrons either on the surface (>1 keV) or within or on the surface of dielectrics deep with the spacecraft (>0.2 MeV), damage to surfaces and thin films (>100 eV ions and electrons), and impacts by micro-meteoroids or space debris. Lower power, light-weight, yet fully capable detectors are required to expand space situational awareness beyond limited data from a few satellites to a robust global picture fed by data from many satellites. Miniaturized space environment sensors on DoD satellites are a necessity for unambiguously identifying the source of anomalous behavior, i. e., whether hostile or natural. Data accumulated from many sensors over long periods of time are essential for building accurate climatological, nowcast, and forecast models, which will improve cost/capability tradeoffs in the satellite design process, improve anomaly resolution, and reduce the risk for operations planning.

2.1. Space Instrument Development

The objective of the space instrument development task is to build, integrate, and space-test advanced detectors to measure the full range of space plasma, energetic particle, micrometeoroid, and debris distributions for space situational awareness. Much of the detailed work is done in collaboration with external contractors, who often build the actual instruments, though the initial concept development, multi-instrument integration, calibration, experimental demonstration, and data reduction are largely carried out by in-house personnel. Data from the instruments are used by AFRL, industry, academia, and other government agencies to perform theoretical and numerical analysis and develop models.

2.2. AF-GEOSpace

AF-GEOSpace is a user-friendly, graphics-intensive master program bringing together many of the space environment models and applications developed over the last 50 years by AFRL, its contractors, and collaborators. The overarching goal of AF-GEOSpace is to provide spacecraft operators, engineers, forecasters, scientists, students, and teachers with software tools to accomplish a wide variety of tasks related to the space environment. The program has grown steadily in an effort to address the concerns of the space weather community, to assist in providing an historical validation baseline for relating models covering similar domains, and to act as a development tool for automated space weather visualization products. The first public release of AF-GEOSpace software, Version 1.21, in 1996, contained radiation belt particle flux and dose models derived from CRRES satellite data, an aurora model, and an ionospheric model plus HF ray

tracing capabilities. AF-GEOSpace Version 1.4 (Hilmer, 1999) included science modules related to the cosmic ray and solar proton environment, low-Earth orbit radiation dosages, single event effects probability maps, and ionospheric scintillation, solar proton, and shock propagation models. New application modules for estimating linear energy transfer (LET) and single event upset (SEU) rates in solid-state devices, and modules for visualizing radar fans, communication domes, and satellite detector cones and links were added. Automated FTP scripts permitted users to automatically update their global input parameter data set directly from the National Oceanic and Atmospheric Administration (NOAA) Space Environment Center. Real-time Defense Meteorological Satellite Program (DMSP) data modules for displaying auroral particle data and identifying enhanced outer zone electron belt populations were also included.

AF-GEOSpace Versions 2.0 and 2.1, developed and released during the period FY02–FY07, contain new science, application, graphics, and data modules, retaining and enhancing the capabilities of the previous releases. AF-GEOSpace serves as a platform for rapid prototyping of operational products, scientific model validation, environment specification for spacecraft design, mission planning, frequency and antenna management for radar and HF communications, and post-event anomaly resolution. Uses of AF-GEOSpace include (1) optimal orbit specification for avoidance of radiation hazards; (2) satellite design assessment and post-event analysis; (3) forecasting of solar disturbance effects; (4) frequency and antenna management for radar and HF communications; (5) determination of communication link outage regions for active ionospheric conditions; (6) specification of meteor flux rates along orbits plus probabilities of incurring damage; (7) display of user formatted space environment sensor data with orbit trajectories; (8) display of DMSP particle spectra and integrated flux from the SSJ4/5 particle sensors; (9) display tools for interpreting MHD simulation results on large-scale structured grids; (10) determination of location of geomagnetic footprints of satellites for conjunction studies; and (11) interplanetary, magnetospheric, and ionospheric physics research and education.

2.3. Spacecraft Charging and Charge Mitigation

Our effort in spacecraft charging technology was focused primarily on the electrostatic charging due to the natural environment but also included other areas of spacecraft plasma interactions where the technology overlap was significant. Altogether these efforts spanned space flight hardware, theory, and simulation. Much of the effort was conducted by contractors, but AFRL personnel were significantly involved in the scientific and technical direction of those efforts as well as in their own independent investigations. Development of the NASCAP-2K simulation code for spacecraft charging, for example, was conducted by SAIC with significant guidance and involvement from AFRL

The Earth's magnetic field traps electrons responsible for both deep dielectric and surface charging of operational satellite systems. With large buildups of charge, these systems are susceptible to rapid electrical discharges, which can cause damage leading to outages. During FY02–FY06 AFRL developed a Satellite Charge/Discharge Product (Char/D) for the Technology Applications Division of the Space and Missile Systems Center at Peterson Air Force Base, Colo. Char/D was designed to combine observations

and modeling of a wide range of electron energies in many magnetospheric regions to create tailored system-impact decision aids related to the specification and forecast of both surface and deep charging of satellites. The product also includes real-time space environment data displays and output from environment models to contribute to general Space Situational Awareness (SSA).

3. TECHNICAL APPROACH

The basic approach is for AFRL personnel to identify technology needs; construct investigations where their effort is significantly leveraged by contactor support; manage the acquisition of knowledge, tools, and instrumentation; and then evaluate and guide the application of the solutions with tests and experiments, including laboratory and space flight demonstrations.

3.1. Space Instrument Development

There are two types of sensors being developed, tested, and flown in this program– those meant to provide situational awareness on operational satellites and those designed to gather data for improved space environment models. Effort on the first type has largely focused on the space demonstration of the Compact Environmental Anomaly Sensor (CEASE) and concepts for the follow-on Space Environment Distributed Anomaly Resolution System (SEDARS). In the second category a suite of space particle instruments is being developed to fly on the AFRL Demonstrations and Science Experiment (DSX) satellite. Typically the science-level sensors produce higher quality data but are heavier and more resource-consuming than the operational sensors. For the next generation of sensors new techniques are also being explored via modeling and laboratory experiments. In particular, significant work has been done investigating a new concept for hyper-velocity impact detectors based on the sensing of both optical signatures and radio emissions from plasmas produced by impacts. Descriptions of these efforts are provided below.

3.1.1. Compact Environmental Anomaly Sensor (CEASE)

The Compact Environmental Anomaly Sensor is a small (10 cm ×10 cm × 8.2 cm), low-power (1.5 W), low-mass (1 kg) instrument package designed to monitor the radiation environment with measurements from its two dosimeters, telescope, and single event effects (SEE) sensor. An electrostatic analyzer (ESA) capability can be added (CEASE-II) to measure low-energy electron fluxes responsible for spacecraft surface charging.

Each dosimeter in CEASE consists of a single solid-state Si sensor located behind an aluminum planar shield. The thin shield (0.08 in) dosimeter has a penetration energy threshold of 20 MeV for protons and 1.2 MeV for electrons. The thick shield (0.25 in) dosimeter has a penetration energy threshold of 35 MeV for protons and 2.5 MeV for electrons. Energy deposited in each dosimeter by each incident particle is measured and the particle is identified in one of three channels: Low Linear Energy Transfer (LoLET,

0.05–0.85 MeV), High Linear Energy Transfer-A (HiLET A, 0.8–3.0 MeV), or High Linear Energy Transfer-B (HiLET B, 3–10 MeV). The telescope consists of two coaxially mounted solid-state Si sensors within a copper casing that is collimated at the top. The collimator is covered with a thin aluminum foil to shield out high fluxes of low energy particles (keV electrons and keV protons). The copper shielding absorbs MeV protons and MeV electrons to minimize unwanted background. Particle species and energy identification is accomplished by analyzing the energy-deposition signatures in the two Si sensors and binning the results into 80 logic boxes.

SEE-type events are measured by a well-shielded sensor, identical to the dosimeters, that responds only to incident particles that deposit large amounts of energy (>50 MeV) in its sensitive volume. Such events can only be caused by the passage of very high-energy protons or heavy ions through the detector. Protons can deposit this amount of energy in the sensors in two ways, either by causing a nuclear interaction in the sensor material or, if their energy is above 50 MeV, by ionizing energy loss while traveling parallel to the long axes in the $0.9 \times 0.9 \times 0.04$ cm detector. Heavy ions, due to their high ionization rates, can deposit 50 MeV in the SEE sensors by ionizing energy loss alone. The measured rates of these events have been found to correlate well with the upset rates of a variety of devices (Mullen and Ray, 1994; Mullen et al., 1995). The CEASE II ESA is a standard cylindrical electrostatic analyzer measuring electrons in the range of 5–50 keV with a 1-second time resolution. Details of the design of CEASE are given by Dichter et al. (1998) and Redus (2003).

CEASE can provide data in three different modes: engineering, science, and history. To provide critical environmental hazard alerts with minimum telemetry, in its engineering mode CEASE generates real-time warnings to the spacecraft operators every five seconds in the form of eight 4-bit hazard registers (HRs) and eight 1-bit warning flags (WFs). The HRs have 16 levels to quantify the level of the environmental threat from zero (lowest level) to 15 (highest level). HRs are constructed from dosimeter, telescope, and SEE detector channels and are designed to quantify the full range of spacecraft hazards, from surface and deep-dielectric charging to total dose and single event effects. The WF provides an alert if an environmental hazard level has exceeded a preset danger threshold, which can be adjusted on-orbit in the light of operational experience. In its science mode CEASE provides a more complete data set suitable for scientific analysis. The data comprise LoLET and HiLET doses and flux counts from both dosimeters, counts from 72 of the 80 telescope logic boxes (some individually and some grouped), and HR and WF flag information. All data are at a five-second measurement resolution. The history mode combines the data of the engineering and science modes in 16 channels with a time resolution of 15 minutes. The data are stored for the previous 72 hours in the instrument and can be called down in the event of a satellite anomaly or WF trigger.

A variety of methods have been used to calibrate CEASE. The dosimeters were calibrated by exposing them to γ-ray radiation from ^{135}Be and ^{137}Cs radioactive sources (LoLET). Higher energy depositions (HiLET) were calibrated by injecting known amplitude test pulses into the dosimeter circuits and comparing the calibrated LoLET

response with HiLET channels (Dichter et al., 1998). Telescope calibration was performed using electron and proton beams at the NASA Goddard Space Flight Center Radiation Effects Facility (Dichter et al., 2006). We have done extensive Monte-Carlo modeling of the instrument response functions, which, together with partial validation by the beam tests, has been essential for the computation of geometric factors for several telescope and dosimeter channels that have been designated the "standard channels" for CEASE. Dividing the channel count rates by the associated geometric factors yields an estimate for the integral proton and electron fluxes needed for scientific analysis of the particle environment.

To validate the performance in space, CEASE has been successfully flown and operated on two satellites and is scheduled to be flown on at least two more. The intent of the program is to exercise CEASE in all space particle environments that could be experienced by operational systems. These include the popular low Earth orbit (LEO) and geosynchronous Earth orbit (GEO) regimes, which are mostly below (LEO) and above (GEO) the Van Allen radiation belts. Between LEO and GEO the inner proton belt and outer electron belt pose more serious radiation hazards to satellites in medium Earth orbit (MEO) and highly elliptical orbit (HEO). A good orbit for efficiently measuring the intense inner and outer belts is a geosynchronous transfer orbit (GTO) which ranges between LEO and GEO near the geographic equator. The initial test plan for CEASE included flights by the Space Test Program (STP) on its Tri-Service Experiment 5 (TSX-5) satellite in LEO, on the Air Force Defense Support Program 21 (DSP-21) satellite in GEO, and by STP on its Space Technology Research Vehicle 1c (STRV-1c) satellite in GTO. Both the TSX-5 and DSP-21 flights were highly successful and will be described in Section 4.1.1. The STRV-1c satellite failed several weeks into its mission, however, and no useful GTO data were returned. CEASE has since been manifested on two more space test satellites, the AFRL Demonstration and Science Experiment (DSX) satellite slated for MEO (6,000 ×12,000 km, 28° inclination) to explore the region between the inner and outer belts, and the Navy Tactical Satellite 4 (TacSat-4) in a small HEO (520 × 1291 km, 63° inclination) traversing the inner belt and slot region. DSX and TacSat-4 will provide the validation of CEASE capabilities in a harsh environment, where data are currently lacking because of the STRV-1c failure.

The Space Environment Distributed Anomaly Resolution System (SEDARS) is envisioned as a follow-on to CEASE and CEASE-II. Major objectives for the SEDARS project are to further miniaturize the sensors and electronics of the particle dosimeters and telescopes, develop a distributed system architecture in which individual sensors could be placed at different optimal locations on the spacecraft yet operate in coordination if need be, and explore the addition of new types of environment and effects sensors. Initially, chemical contamination and hyper-velocity impact (e.g. from micro-meteoroids and space debris) detectors were considered. Subsequent discussion with AF, DoD, NASA, and Aerospace Corporation groups responsible for satellite protection and situational awareness has indicated that surface charging, internal discharging, and hyper-velocity impact monitors are the highest priority for new capabilities. With the advent of the DSX mission and the responsibility of the Space Particles program to develop a large fraction of the needed space environment sensors (Section 3.1.2) there have not been

resources available to fully pursue SEDARS during the past few years. However, significant effort has gone into exploring a unique concept for hyper-velocity impact detection, described in Sections 3.1.3 and 4.1.3, which, if successful, could eventually be incorporated into SEDARS.

3.1.2. Space Particle Instruments on the Demonstration and Science Experiment (DSX) Satellite

The radiation belt "slot" region is so named because early observations, represented by the NASA AP-8 and AE-8 radiation belt models, for example, indicated a paucity of energetic particles in comparison to the inner and outer belts. (The slot lies between L-shells of approximately 2 and 3. An L-shell is a surface along magnetic field lines that at the magnetic equator are the specified number of Earth radii from the Earth's center.) Observations over the last few solar cycles, however, have indicated that the slot region is far from quiescent. Particle populations vary widely with magnetospheric wave and convection electric field activity. An extreme example was the March 1991 geomagnetic storm, which created intense new belts that lasted for months. To better characterize and understand the dynamics of the slot region AFRL is developing the Demonstrations and Science Experiment (DSX) satellite for flight in 2010 with a nominal $6{,}000 \times 12{,}000$ km, mid-inclination orbit. DSX will carry several science payloads designed to (1) measure the distribution of energetic particles, plasmas and electromagnetic fields, (2) validate models of Very Low Frequency (VLF) wave propagation and wave-particle interactions, and (3) investigate radiation effects on advanced spacecraft technologies. Detailed descriptions of the DSX bus and payloads are given by Spanjers et al. (2006).

It is imperative that sound measurements be made of the plasma and energetic particles so that adequate climatological, situational awareness, and forecast models can be developed to enable the successful design and operations of DoD space systems in these new and desirable MEO regimes. Specific deficiencies of current standard radiation belt models in the inner magnetosphere include the lack of (a) spectrally resolved, uncontaminated measurements of high energy protons (10–400 MeV) and electrons (1–30 MeV) and (b) accurate mid to low energy (< 1000 keV) measurements of the energetic particle and plasma environment. The space weather instruments and the unique orbit of DSX are designed to address these deficiencies. Accurate environment determination is also important for DSX itself, so that quantitative correlation with the performance of the spacecraft and its payloads over the course of the mission can be made.

We are developing five space particle detectors for DSX, several with the capability of measuring both the spectral content and angle of arrival of electrons and protons over broad energy ranges. An on-board magnetometer (supplied by another program) will allow for the transformation of angle-of-arrival measurements into estimates of the flux distribution with respect to the local pitch-angle, i. e., the angle between the particle velocity and magnetic field. Local pitch-angle distributions can then be used to estimate global particle distributions by mapping techniques using the well-known equations of motion and magnetic field models tagged to the local measurements. A description of the individual sensors is given below.

1. Compact Environmental Anomaly Sensor (CEASE). Section 3.1.1 contains a description of CEASE capabilities. The angular field-of-view for CEASE is relatively large and will not allow for pitch angle resolved measurements. However, in addition to electrons and protons it will measure dose rates and single event effects. One change for the DSX CEASE compared to units previously flown is that the sensor will capture and downlink the full dose spectra from each dosimeter, whereas prior versions captured only six reduced data points (two for LoLET data and four for HiLET data). CEASE was developed under AFRL contract by Amptek, Inc., and is being tested and integrated into DSX by AFRL and Assurance Technology, Inc.

2. Low Energy Electrostatic Analyzer (LEESA). LEESA will measure fluxes of low energy electrons and protons spectrally resolved in the range 30 eV to 50 keV. The directionality of the incoming particles will be determined by measuring in five angular zones spanning 120° in the plane containing the magnetic field with an approximate 4° width in the direction perpendicular to the look-plane containing the magnetic field. These low energy particles constitute the "space plasma" and are responsible for surface electric charging and damage to thin films such as thin-film photovoltaics, conventional solar cell cover glasses, and coatings. LEESA is being built in-house by AFRL.

3. Low Energy Imaging Particle Spectrometer (LIPS). LIPS is designed to measure the "ring current" particles that are important contributors to the energy flow processes in the magnetosphere. This particle population also plays an important role in spacecraft charging and surface damage due to sputtering. The instrument uses specially designed combinations of scintillator materials to detect electrons and protons with energies between 20 keV and 1 MeV. Eight 10° × 8° field-of-view windows will provide pitch angle resolution. LIPS is being developed under AFRL contract by Physical Sciences, Inc.

4. High Energy Imaging Particle Spectrometer (HIPS). HIPS will measure electrons with energies of 1–10 MeV and protons with energies of 30–300 MeV. The field of view will be 90° × 12.5° resolved in eight angular bins along the large angle direction. These high energy particles are responsible for microelectronics damage, displacement and total dose damage, SEEs, and deep dielectric charging. HIPS is being developed under AFRL contract by Physical Sciences, Inc.

5. High Energy Proton Spectrometer (HEPS). Accurate measurement of high-energy proton populations (>100 MeV) in the near-Earth space environment is a challenge because of the contamination caused by other high energy particle populations, which include electrons, cosmic rays, etc., as well as protons outside of the measurement range of interest. Consequently, few reliable measurements exist. The operational consequences of this population are important, because the highest energy protons penetrate deeply into a space vehicle to reach even heavily shielded components and cause nuclear activations and single event effects. HEPS is designed to measure protons in the energy range 20–440 MeV in 22 logarithmically spaced channels. Measurement issues are addressed through the use of (a) a unique combination of thin semiconductor

detectors and a thick segmented scintillation detector (made from a new material) to improve the measurement accuracy of incident proton energies, (b) a combination of active coincidence requirements and passive shielding to reduce the response to large omni-directional and directional fluxes impinging on all sides of the instrument, and (c) a flexible on-board data processing system that can be used to focus not only on the particles of interest, but also on other physical effects of particle penetrations in matter to include inelastic nuclear scattering, straggling, out-of-band contamination, out-of-aperture contamination, etc. It has a 12° full-cone field of view, sufficiently small to resolve details of the pitch-angle distribution, albeit one point at a time. Although originally designed to measure protons, it also includes several data channels for measuring background events and 20 channels for measuring electrons above ~1.5 MeV. HEPS is being developed under AFRL contract by Assurance Technology, Inc., with design and validation assistance provided by AFRL.

3.1.3. Hypervelocity Impact Detectors

In 2003 a small project was initiated to evaluate the magnitude of radio frequency interference (RFI) generated by debris plasma from hypervelocity impacts to spacecraft, with the hope that the interference would be of sufficient magnitude to reliably detect. After a careful review of the literature, it was determined that a well-supported estimate of the RF emissions from impact plasmas could not be made using available reports or existing models. AFRL therefore contracted with the Sandia National Laboratories (SNL) at Kirtland Air Force Base, N. M., in 2004 to conduct hypervelocity launches between 1 and 19 km sec^{-1} in an attempt to measure actual emissions from debris plasmas. Although the magnitude of the debris plasma emissions proved to be essentially undetectable, the RF emissions from the impact itself quickly showed themselves to have potential for remotely detecting impacts to spacecraft from micrometeoroids, orbital debris, and kinetic kill weapons, thereby filling a critical Space Situational Awareness need.

Motivated by these early results, we initiated a project to develop an instrument for remotely sensing impacts to spacecraft using a combination of radio frequency and optical emissions. Experiments with hypervelocity launchers at SNL in 2004, 2006, and 2007 demonstrated easily detectable electromagnetic emissions spanning (at least) the band from DC to 18 GHz. In addition, concurrent work by Maki et al. (2005) demonstrated detection at 22 GHz. These measurements enhance longstanding and ongoing efforts by NASA and others to characterize the optical flash from impacts. Although optical flash detectors may seem an obvious choice for use as impact detectors on spacecraft, in reality a host of confounding factors, including solar glint and contamination and line-of-sight requirements, make a practical implementation difficult. By combining a radio-frequency detection system with an optical localization system, a multi-band sensor could dramatically enhance space situational awareness. In addition, careful consideration of optical flash rise times and emission spectra can yield impactor velocity and composition and assist with impact characterization and possibly attribution. AFRL is continuing laboratory testing with the goal of producing a design for a miniaturized impact detector suitable for space test.

3.2. AF-GEOSpace

AF-GEOSpace Version 2.1 is an object-oriented code written in C++ for WindowsXP and LINUX systems. It is rigorously object oriented and contains separate user interface, kernel, and graphics libraries. The software is divided into five explicit module classes to simplify the integration of new algorithms and increase portability. *Science Modules* control individual science models and produce output data sets on user-specified grids. *Application Modules* typically manipulate these data sets, e.g., by integrating dose calculated by a radiation belt model or tracing HF rays through a model ionosphere. Application modules also provide orbit generation and magnetic field line tracing capabilities. *Data Modules* read and assist with the analysis of user-generated and DMSP data sets. *Graphics Modules* control the one, two, and three-dimensional windows and enable display features such as plane slices, magnetic field lines, line plots, axes, the Earth, stars, and satellites. *Worksheet Modules* provide commonly requested coordinate transformations and a calendar system conversion tool.

3.3. Spacecraft Charging and Charge Mitigation

3.3.1. NASA-Air Force Spacecraft Charging Analyzer Program (NASCAP-2K)

Spacecraft charging is a phenomenon for which the basic physics has mostly been understood for decades, but for which the transition to an engineering capability requires high-fidelity Computed Aided Design (CAD) and simulation. NASCAP-2K Version 2.0 is a three-dimensional computer code used to model interactions between spacecraft surfaces and plasma environments in low Earth orbit, geosynchronous orbit, auroral regions, and interplanetary space, including plasmas emitted from spacecraft sources. Features include a native object builder and 3-D graphics; external geometry input from common mechanical CAD software; particle and field solutions in dense, rarefied, and flowing plasma; particle-in-cell (PIC) time dependent plasma analysis; extensive material properties; and system generated plasma plumes such as from electric thrusters or charging control devices. Currently implemented are: (1) an Object Definition Toolkit; (2) the Boundary Element Method (BEM) for calculating surface charging in geosynchronous Earth orbit, solar wind, or other tenuous plasma environments; (3) a graphical interface for setting up problems and examining results; (4) a new GridTool program for dense plasma problems that require a gridded solution; (5) a PIC capability with a continuously variable time step that extends from explicit PIC at short time steps to a steady state implicit method at long time steps, with a variety of hybrid capabilities in between. When an electric field solution is required for problems involving dense plasma, a non-linear finite element method is employed, which guarantees continuous electric fields, in contrast to most linear methods that result in piecewise continuous potential but discontinuous electric fields, which can lead to noisy or even unstable solutions.

NASCAP-2K and predecessor models have a long history of successes both in commercial use to design charging-tolerant spacecraft and in interpreting the results of space experiments. Mandell et al. (2004, 2005, 2006) presented descriptions of the code and its capabilities. While the code is not used operationally, it is used during the

spacecraft design phase and employs idealized representations of the space environment, e.g., worst-case Maxwellian particle distributions. NASCAP validation work using early versions of the spacecraft charging codes (Stannard et al., 1982; Katz et al., 1983) helped establish baseline capabilities. A more recent validation summary for NASCAP-2K spacecraft-environment interactions calculations was provided by Davis et al., (2004). This validation established the accuracy of the code by comparing computed currents and potentials with analytic results and with published calculations using earlier codes. Among other successful comparisons, NASCAP-2K predicts Langmuir-Blodgett current collection at geosynchronous altitude and predicts the same current as a function of applied potential as was observed for the SPEAR I rocket in the low Earth orbit regime. NASCAP-2K represents the current state of the art in spacecraft charging codes.

3.3.2. Satellite Charge/Discharge Product (Char/D)

While several models and applications have been developed for this product, the simple display of real-time environment and satellite data still represents the most robust, although not system-specific, method for providing SSA. Real-time space environment indices processed and displayed by this product include: the planetary magnetic index ap, the daily-averaged Climax Neutron Count Rate, the auroral equatorward edge boundary at midnight and cross-polar cap potential drop (both derived from DMSP particle data), the geomagnetic activity index Kp and the daily sum of 3-hour values, the Polar Operational Environmental Satellite (POES) Belt Index (PBI) values, the daily sunspot number, and the Thule Neutron Count Rate. Real-time spacecraft data displayed and used as input to the models include (1) solar wind magnetic field, particle density, and velocity values from the Advanced Composition Explorer (ACE); (2) precipitating electron and ion spectrometer fluxes from the DMSP SSJ4/5; (3) ion scintillation monitor measurements of plasma density, temperature, and velocity from the DMSP SSI/ES; (4) energetic electron and ion fluxes from the Los Alamos National Laboratory (LANL) Energetic Spectrometer for Particles (ESP), Magnetospheric Plasma Analyzer (MPA), and Synchronous Orbit Particle Analyzer (SOPA); (5) energetic electron and ion fluxes from the NOAA Geostationary Operational Environmental Satellite (GOES) Energetic Particle Sensor (EPS); and (6) electron fluxes from the NOAA POES Medium Energy Proton/Electron Detector (MEPED).

3.3.3. Spacecraft Charge Detection and Mitigation

Other activities in spacecraft charging focused on instruments to detect charging and technologies for mitigation. An improved Compact Environmental Anomaly Sensor (CEASE-II) was built by Amptek, Inc., and has been flying on the DSP-21 satellite since August 2001. Two additional units have been sold to commercial satellite developers. The principal improvement of CEASE-II over CEASE-I was the addition of a miniature electrostatic analyzer (ESA) to monitor the fluxes of electron in the 0.3 to 30 keV range that cause charging. Responsibility for manufacture and technical support of CEASE was acquired by Assurance Technology, Inc., in 2006.

In addition to the measurement and modeling of satellite charging, we have developed approaches to charge mitigation. One such device, Charge Control System-II

(CCS-II), was built by the Electric Propulsion Laboratory of Monument, Colo. Delivered for evaluation in 2003, it is a compact version of the original CCS, which was flown successfully in 1995 by the Defense Satellite Communications System (DSCS) on its geosynchronous satellite DSCS-III B-7. CCS-II functions by the emission of a xenon plasma from a hollow cathode electron emitter coupled with a secondary ionization chamber. The resulting flux of ions serves to neutralize differential charging and also neutralize the escape of electrons that discharge the frame potential of the spacecraft. After some delay CCS-II is scheduled for testing in a laboratory vacuum chamber in 2008.

Another mitigation approach is the Ion-Proportional Surface Emission Cathode (IProSEC), which is being developed as a partnership between AFRL and MIT Lincoln Laboratory. IProSEC (Figure 1) is a large area, low brightness, passive cathode material that can emit electrons without a neutralizing ion component. Although this approach does not provide ions that could neutralize differentially charged surfaces, it is known that in some configurations this is not necessary. An example is a configuration in which the satellite frame potential will carry the photovoltaic arrays with it to high negative potential, while at the same time the array cover glasses remain at low potential due to the emission of photoelectrons, resulting in dangerous electric fields. Emission of electrons would reduce the frame potential and ameliorate the problem. IProSEC offers the possibility of a totally passive mitigation of spacecraft charging.
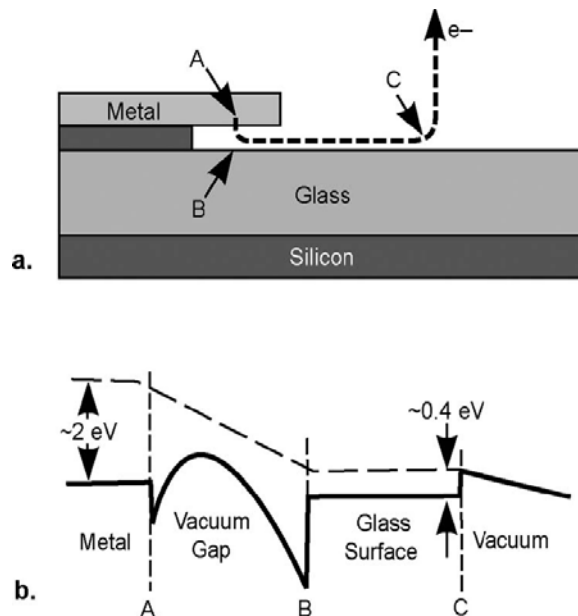
Figure 1. Schematic cross section, not to scale, of a surface emission cathode and potential energy of emitted electron. (a): Broken line denotes a possible emission path with positions marked where the electron is (A) in the cathode, (B) on the glass surface under the cathode, and (C) on the glass surface either exposed to ambient plasma or under an anode (not shown). (b): Solid curve is the potential energy of the electron on its emission path, labeled with the corresponding points A, B, and C. Broken line is the potential energy of an electron in vacuum. These curves assume the work function of the tungsten cathode is 2 eV (Geis et al., 2005).

Electric propulsion is closely related to spacecraft charging. By their very nature, electric propulsion devices have a potential impact on spacecraft charging. Any charging is typically eliminated through use of a neutralizer, but the mechanism through which the neutralizing electrons couple with the thruster's plume of ions is poorly understood. In order to provide better understanding of ion plume-electron coupling, we investigated the potential coupling mechanisms through PIC simulation and theory. Improved understanding of the coupling mechanisms may enable the development of electric propulsion devices that function as charge control devices and may also lead to improvements in other charge control devices such as the CCS-II and IProSEC.

4. RESULTS

4.1. Space Instrument Development

4.1.1. CEASE

On 7 Jun 2000 the first CEASE was launched by the DoD Space Test Program (now the Space Development and Test Wing) on its Tri-Service Experiment-5 (TSX-5) mission into a 410 × 1710 km, 69° inclination low Earth orbit. Turned on one day later, the instrument was in continuous operation until 3 Aug 2006, completing more than 30,000 orbits of the Earth. The mission was highly successful in demonstrating the capabilities of CEASE for both anomaly resolution and generation of scientific-caliber data for space environment model construction. Figure 2 shows the space environment over the entire TSX-5 mission as seen by two standard CEASE dosimeter channels measuring mostly >1 MeV electrons (Figure 2a) and 37–42 MeV protons (Figure 2b), respectively. CEASE on TSX-5 was witness to a wide range of space environment conditions in the time period spanning the maximum of solar cycle 23, including some of the most intense solar proton events ever recorded (October 2003 and January 2005) and the most intense relativistic electron event ever seen by the GOES satellite space environment monitor (July 2004) in more than three decades of operation.

CEASE was called into anomaly resolution service early in its mission when the TSX-5 fiber-optic gyroscope (FOG), a part of the attitude control system, suffered a number of anomalies during the mission, causing the space vehicle to lose attitude knowledge and go into a tumbling mode. It was thought the problem might be related to single event effects caused by energetic protons. An analysis was done using data from the SEE detector on CEASE. A plot of the locations where the anomalies occurred is shown in Figure 3, together with a map of the hazard register data from the SEE detector (HR6). It is evident that all but one of the FOG anomalies occurred in the region of high HR6 values, validating the utility of this HR. In the case of the TSX-5 orbit, the high HR6 region corresponds to the South Atlantic Anomaly, which can be predicted by models.
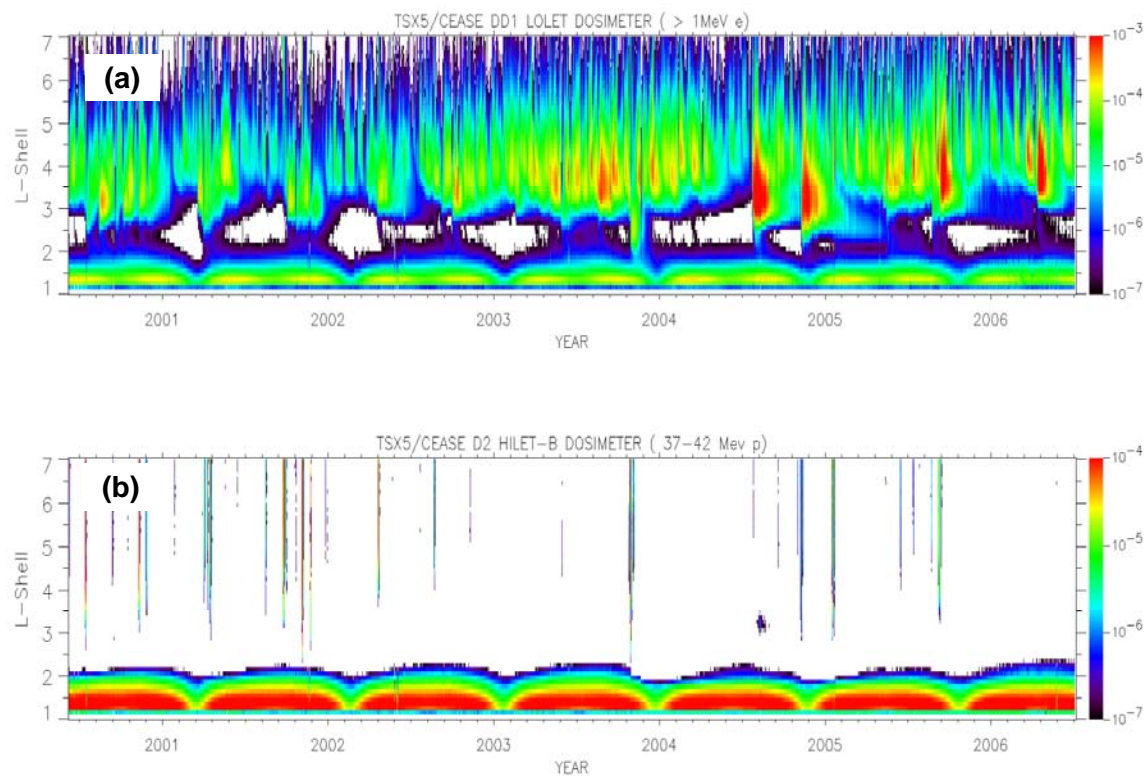
Figure 2. Dose rate [rad(Si) sec^{-1}] averaged over five seconds for the entire TSX-5 mission from two CEASE dosimeter channels measuring mostly (a) >1 MeV electrons and (b) 37–42 MeV protons.
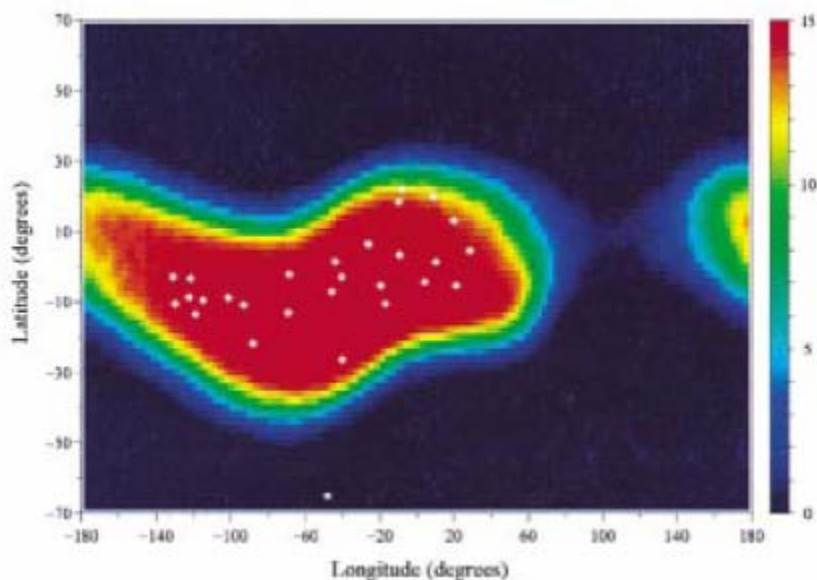
Figure 3. Map of Single Event Effect (SEE) hazard register HR6 values from CEASE on TSX-5. Color scale denotes relative probability of single event effects. White stars mark locations of occurrences of anomalies of the TSX-5 fiber-optic gyroscope (from Dichter et al., 2001).

An additional use of CEASE data in addressing issues of radiation effects on component or subsystem performance is illustrated by a further analysis of the FOG data. Using data from the CEASE telescope, it can be shown that the observed FOG upsets are correlated with the high-energy proton flux (E > 30 MeV) and the sensitivity of the devices to proton damage can be determined. If the SEE upsets are caused by rare, large energy deposition interactions due to high-energy protons, then the time rate of device upsets R is proportional to the flux of high-energy protons F, i. e., $R = kF$, where k is the susceptibility of the device to upset. The device susceptibility can be determined either prior to flight by particle beam testing or in flight using observed upset rates and measured particle fluxes, such as those available from CEASE. Figure 4 shows a plot of the observed FOG upset rate against the E > 30 MeV proton flux levels as measured by CEASE, where the upset rate at a given flux level is the number of observed upsets at that flux level divided by the time that the spacecraft was exposed to that flux level. Error bars indicate the one standard deviation statistical uncertainty associated with the observed upset counts assuming Poisson statistics. The observed linear relationship, with zero offset and a constant of proportionality of ~1.9 x 10^{-9}, is what is expected if the high-energy protons are responsible for the FOG upsets. This type of analysis has significant utility in that it allows a quantitative post-anomaly investigation of the environmental causes of a problem. Both the particle population responsible for the effect and the quantitative level of sensitivity of the component or subsystem to this population can be determined. More examples of CEASE data being used for space environment hazard analysis on TSX-5 were presented by Dichter et al. (2001).

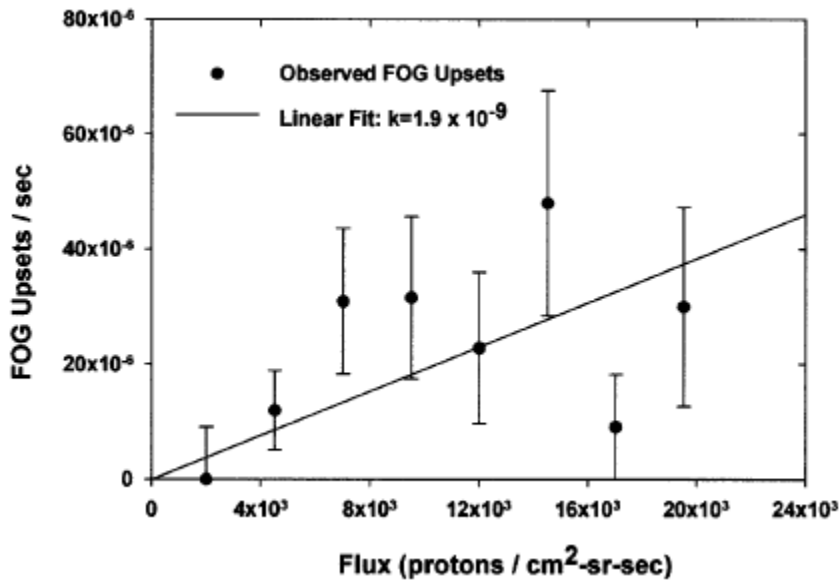Figure 4. Observed TSX-5 fiber-optic gyroscope upset rate as function of E > 30 MeV proton flux. Error bars are one standard deviation statistical uncertainties associated with the observed counting rates. Solid line is a linear fit to the data.

The orbit of the TSX-5 satellite and duration of the mission made data from CEASE especially useful for characterizing the low Earth orbit radiation environment over an

altitude range relevant to many DoD LEO constellations. Several anomaly studies were done for DoD customers using CEASE data taken near the time of the anomalies when CEASE was in magnetic coordinate conjunction with the subject vehicle, i. e., on the same L-shell and position along the magnetic field line but not necessarily the same magnetic longitude. New climatological models of both energetic proton and electron distributions applicable to satellite design have been developed using the integral flux data derived from the CEASE standard channels (Metcalf et al., 2007; Brautigam et al., 2001, 2004; Ginet et al., 2007a, 2007b).

On 6 Aug 2001 the first CEASE-II unit was launched onboard the Defense Satellite Program 21 (DSP-21) satellite into geosynchronous orbit. It continues in operation as of this date. Figure 5 shows the daily averaged data from two standard CEASE dosimeter channels corresponding to measurements of approximately >1 MeV electrons (Figure 5a) and 37–42 MeV protons (Figure 5b) over an approximate 200-day period beginning 11 Aug 2001. Also shown in red is the daily averaged response of the same two channels on the TSX-5 satellite in LEO. Examining the electron behavior (Figure 5a), we see that the flux intensity on average is significantly greater at GEO than at LEO though the general trend of increasing and decreasing is mirrored. This is expected since energetic electrons are injected and accelerated near the magnetic equator in the tail regions of the Earth's magnetosphere, where CEASE/DSP-21 measures them, but are scattered due to wave-particle interactions and electric and magnetic field fluctuations before they get to lower altitudes where CEASE/TSX-5 measures them. Protons, on the other hand, show almost identical flux levels between LEO and GEO (Figure 5b) during solar proton events (SPEs) and background levels at GEO outside the event intervals. The absence of CEASE/TSX-5 measurements during SPEs is a result of TSX-5 being at lower latitudes, where it is unable to measure the solar protons streaming in at the higher latitudes. Between SPEs the background counting rate on the CEASE/TSX-5 channel is less than 1 per 5 sec. A more extensive comparison of several CEASE proton-sensitive channels on DSP-21 and TSX-5 during all the SPEs from Aug 2001–Jul 2006 has found ratios of count rates between 0.8 and 1.3, a strong indication that both detectors are working as designed. CEASE proton fluxes from DSP-21 have also been compared to the "community standard" measurements made by Space Environment Monitor on the GOES satellites with good agreement (Golightly and Knorring, 2005).

CEASE-II/DSP-21 extended the CEASE capability by including an electrostatic analyzer designed to measure electrons in the range 5–50 keV. At GEO electrons in this energy range are abundant and a well-known instigator of spacecraft surface charging problems. A spectrogram of the differential flux of electrons measured by CEASE-II during the first 200 days of operation is shown in Figure 6a. In Figure 6b the variation of the geomagnetic Kp index is plotted. Variation of the electron flux clearly tracks variation in Kp, as it should since the electrons in this energy range are associated with the geomagnetic substorms and current systems producing the Kp index. Cross-calibration of the CEASE-II ESA data with measurements from long-heritage ESAs on the LANL GEO satellites is an important validation exercise that remains to be done.
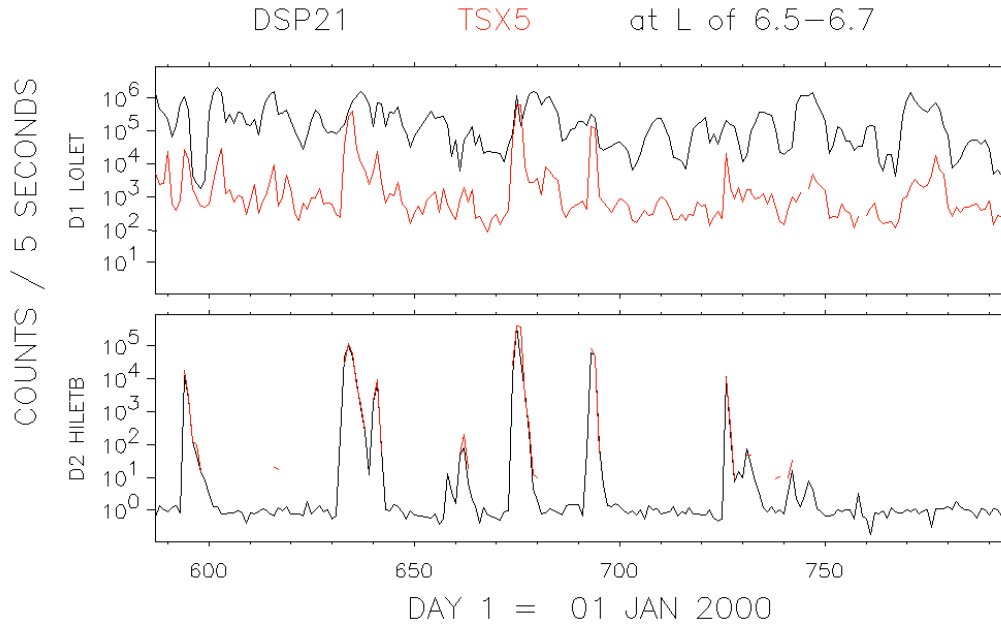
Figure 5. Daily averaged count rates [counts per 5 sec] for an approximate 200 day period beginning 11 Aug 2001 from CEASE channels measuring mostly >1 MeV electrons (a) and 37–42 MeV protons (b) on the DSP–21 (black) and TSX-5 (red) spacecraft.
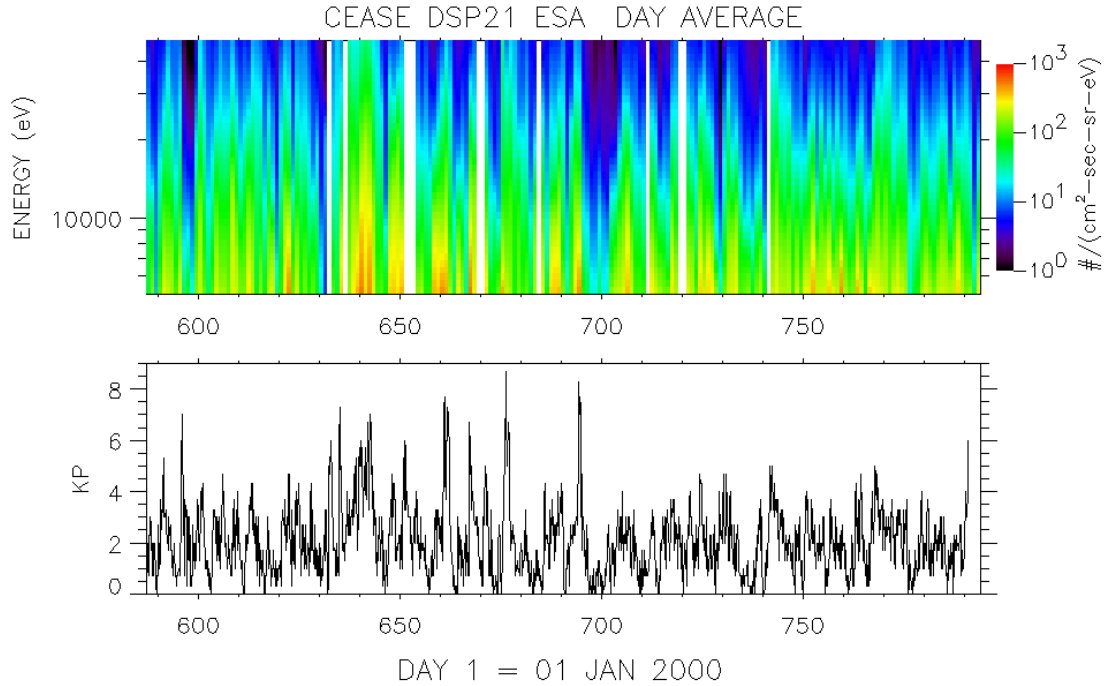
Figure 6. Spectrogram of the CEASE-II electrostatic analyzer daily-averaged electron flux data for the first approximately 200 days of DSP-21 operations (a) and the geomagnetic planetary index Kp (b) for the same time period.

17

CEASE-II was an Air Force Advanced Concept Technology Demonstration (ACTD) meant to "demonstrate the military utility of a small, low-power, on-orbit space weather sensor" (CEASE-II ACTD Final Report, 2004). Displays of CEASE output are in use at the 2nd Space Weather Squadron, Buckley AFB, Colo., which is the squadron responsible for DSP-21 operations. Of major interest to the operators has been the tracking of single event effects. An example of a relevant CEASE-II display is given in Figure 7, where SEE hazard register output (green diamonds) is plotted together with science data output from one of the CEASE-II telescope channels sensitive to energetic protons (red line) during the great solar proton event of October 2003. DSP-21 experienced numerous SEE-related anomalies in this period whose cause was quickly confirmed with the CEASE-II data.

As part of the ACTD a Military Utility Analysis of CEASE-II was performed at the Defensive Counterspace Test Bed (DTB), Schriever AFB, Colo., on 8–13 September 2003 with over 25 space operators and engineers participating. Actual DSP-21 telemetry data were used but modified to contain signatures of space weather and radio frequency interference threats. Operators concluded that (a) CEASE supports space situational awareness, (b) space weather data that are easy to understand should be part of a command and control system that depicts a common operating picture, (c) real-time, high-confidence assessments of the space weather environment are valuable, (d) CEASE supports anomaly resolution procedures, (e) future space policy should state that a CEASE-like capability must be included on future satellite acquistions, and (f) a space weather Concept of Operations (CONOPS) needs to be developed and integrated into space operations.

4.1.2. Space Particle Instruments on the Demonstration and Science Experiment (DSX) Satellite

As of 30 September 2007 all the space particle sensors described in Section 3.1.2 had passed their Critical Design Reviews (CDR) with the exception of LEESA [CDR was completed in February 2008]. Instrument providers are on track for delivery by October 2008, after which integration and test on the spacecraft bus will proceed, with a target date of launch readiness in November 2009. Launch opportunities are being pursued by AFRL and the Space Development and Test Wing (SDTW) with current focus on the possibility of being a secondary payload on DMSP Flight 19, scheduled for early 2010.

4.1.3. Hypervelocity Impact Detector

As reported in Starks et al. (2006), early efforts for this project were designed to address RFI concerns related to debris plasma. For this purpose, broadband radio frequency detectors operating from DC to 1 GHz were placed behind the target material, where they could detect emissions from the debris plasma but not from the impact itself. Nevertheless, because signals from the impact were recorded in some of the higher velocity tests, the experiment was redirected. HF and L-band antennas were added in front of the target material, and they acquired substantial prompt emissions during impacts at 1, 3, 5, 7 and 11 km sec^{-1}. An example of the radio frequency emissions is

shown in Figure 8. In addition, a silicon diode detector and visible and near-IR spectrometers operated by SNL measured and characterized light output at each velocity. In later shots, a quadrature Langmuir probe (QLP) was used to estimate the magnitude of the resulting debris plasma. These measurements clearly established that sufficient radio frequency emissions are produced by hypervelocity impacts to construct an impact detection system, and furthermore that sufficient optical energy is present at all velocities to facilitate impact localization within the field of view.
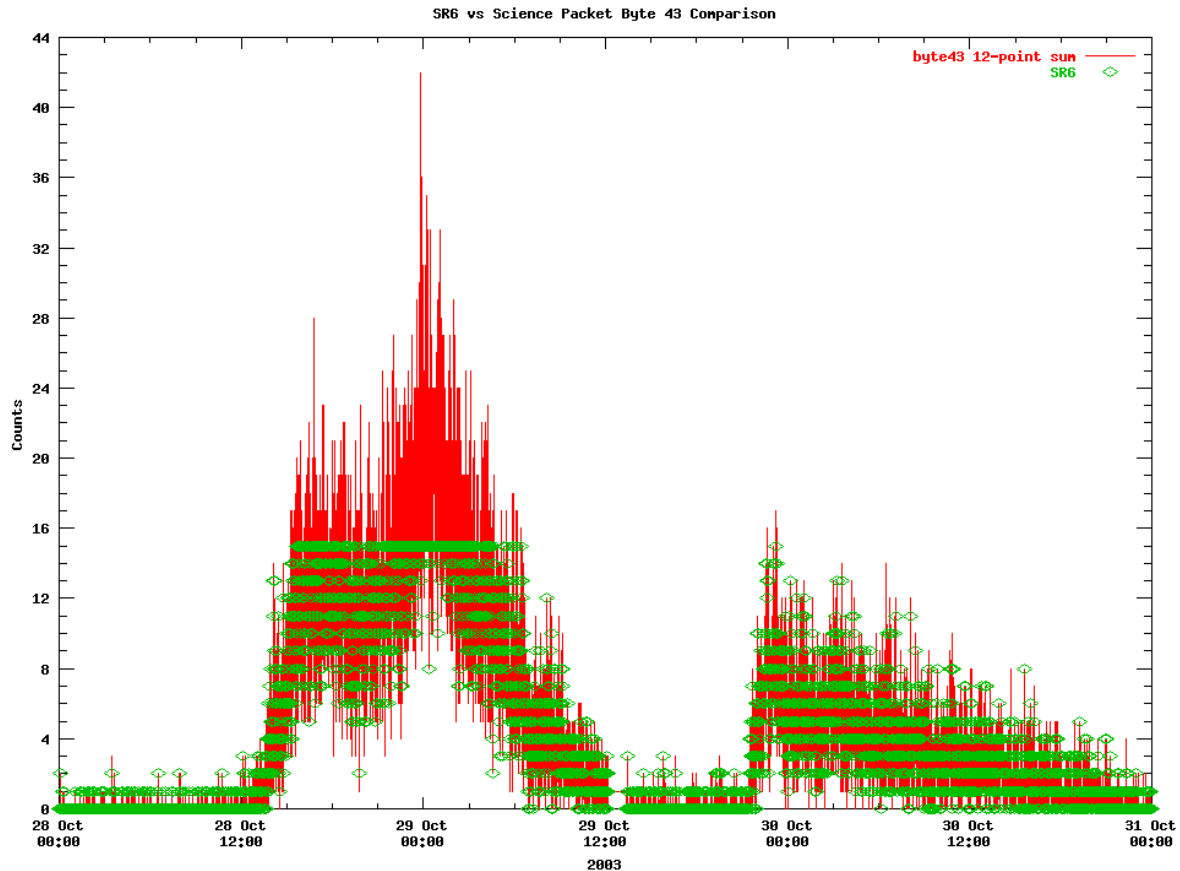
Figure 7. CEASE-II output display showing the single event effect hazard register output (green) and counts per 5-sec interval from a telescope channel sensitive to energetic protons (red) during the October 2003 "Halloween" geomagnetic storm.

Follow-on experiments will deploy a narrow-band microwave detection system operating at 12, 24, and 36 GHz to examine the shorter wavelength radio emissions and provide a path toward miniaturized detectors. In addition, a CCD optical array will be used to provide proof-of-concept localization of the impact. Additional QLP plasma probes will be deployed to further characterize the debris plasma. Finally, the next set of experiments will take place in a high vacuum system for the first time, enhancing the direct applicability to the space environment. The remaining project schedule has been designed to mature the diagnostic system toward a miniaturizable concept flight instrument.
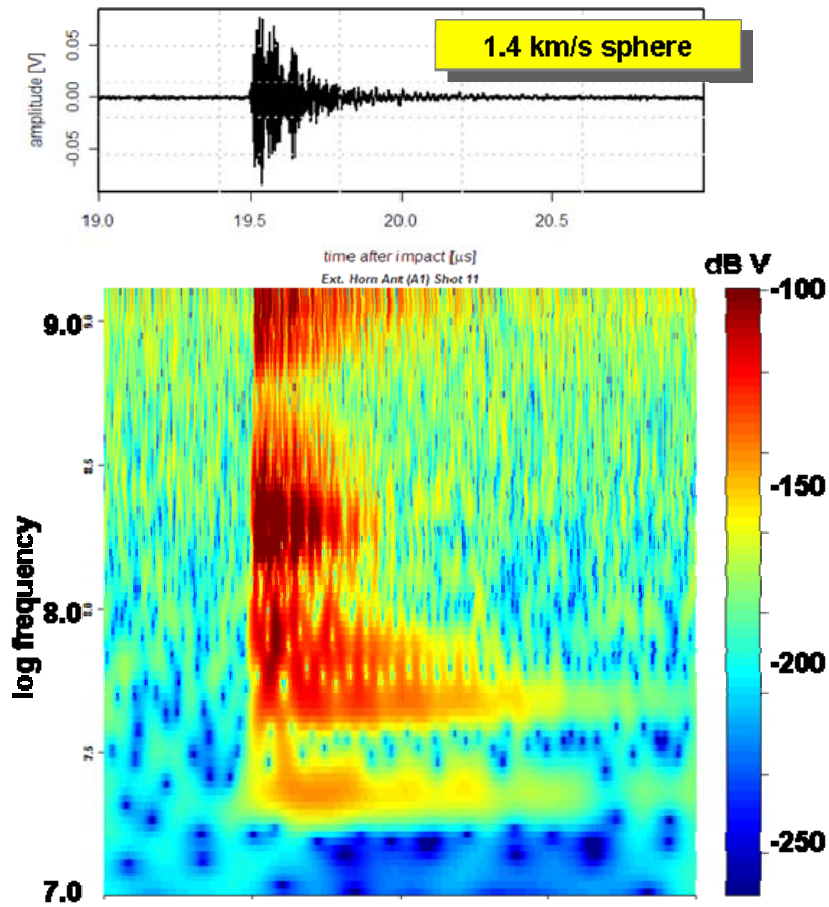
Figure 8. Time series of RF emission from 1.4 km sec^{-1} impact (top) and wavelet decomposition of the signal in frequency space (bottom).

4.2. AF-GEOSpace

Efforts during FY02–FY07 resulted in the release of AF-GEOSpace Version 2.0 (Hilmer, 2002; Hilmer et al., 2004) and AF-GEOSpace Version 2.1 (Hilmer, 2006c) to U.S. Government agencies and their contractors (Distribution Statement C). Because of the sensitivity of some of the content, public release versions with a reduced number of modules were configured and distributed under the headings Versions 2.0P and 2.1P (Distribution Statement A).

AF-GEOSpace Version 2.0 for WindowsNT/2000/XP and LINUX included the first true dynamic run capabilities and offered new and enhanced graphical and data visualization tools such as 3-D volume rendering and eclipse umbra and penumbra determination (Hilmer, 2002). The dynamic run capability enabled the animation of all model results, in all dimensions, as a function of time. Version 2.0 also included a new

realistic day-to-day ionospheric scintillation simulation generator (IONSCINT), an upgrade to the WBMOD scintillation code, a simplified HF ionospheric ray tracing module, and applications built on the NASA AE-8 and AP-8 radiation belt models. User-generated satellite data sets could be visualized along with their orbital ephemeris. A prototype tool for visualizing MHD model results stored in structured grids provided a hint of where future space weather model development efforts are headed. A new graphical user interface (GUI) with improved module tracking and renaming features greatly simplified software operation. Finally, a major restructuring of the code to an open architecture greatly increased the code's portability and made it easier in integrate new modules.

The latest in the line of AF-GEOSpace software releases, Version 2.1, serves as a platform for rapid prototyping of operational products, scientific model validation, environment specification for spacecraft design, mission planning, frequency and antenna management for radar and HF communications, and post-event anomaly resolution. It provides common input data sets; application modules; and 1-D, 2-D, and 3-D visualization tools for all of its models. Available graphical tools include animation, annotation, axes, coordinate probes, coordinate slices, detector cones (e. g., from satellites), Earth, emitters (e.g., radar fans and communication domes), field-lines (e.g., geomagnetic), global inputs (e.g., Kp and Dst indices), grids, isosurfaces, links (e.g., ground-to-satellite), orbit probe (data along orbit tracks), orbit slice (data in orbit plane), plane slice (data in arbitrary plane), ray trace (through ionosphere electron densities), satellites, stars, stations, and volume (global 3-D rendering of data sets). The "dynamic" mode of the software enables the simultaneous display of output from multiple environment models as a function of time over user-specified intervals.

AF-GEOSpace Version 2.1 for Windows/XP and LINUX built on Version 2.0 with the new or improved modules described below. The basic scientific algorithms used to generate the first six of these modules were developed by AFRL scientists and contractors. Appendix A contains brief descriptions of all the science and application modules in AF-GEOSpace Version 2.1. Complete descriptions and model references are contained in the user's manual (Hilmer, 2006c). Figure 9 is an example of the visualization capability of AF-GEOSpace.

(1) Updates to the IGRF internal portion of the magnetic field module (BFIELD-APP),
(2) An application to trace geomagnetic field lines from single user-specified points or multiple points along a satellite orbital track (BFOOTPRINT),
(3) A model providing cutoff rigidity values for solar protons and cosmic rays (CUTOFF),
(4) New DMSP data and graphic modules,
(5) The meteor impact map science model, which calculates the hourly meteor impact or damage rates (METEOR IMPACT),
(6) A meteor sky map module to calculate the number of visible meteors from active meteor showers (METEOR SKY MAP),
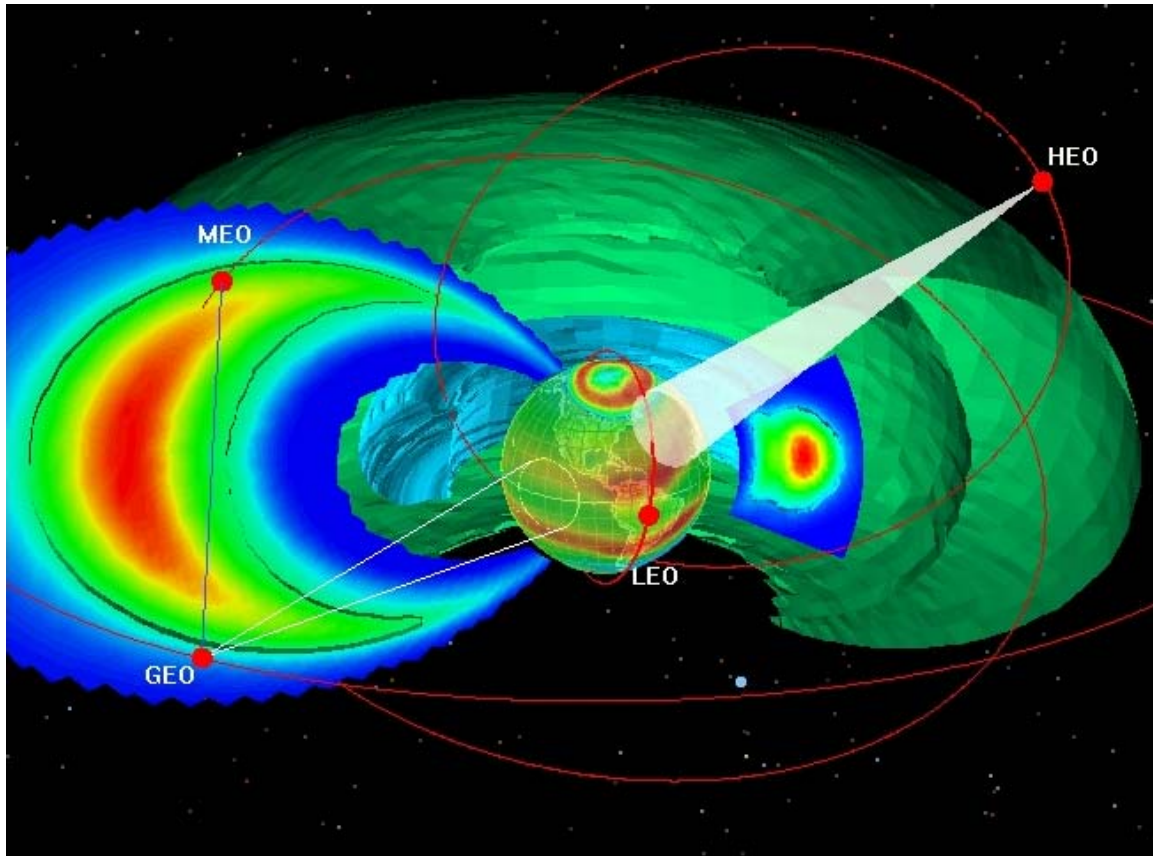
Figure 9. AF-GEOSpace visualization of electron (outer) and proton (inner) radiation belts along with spacecraft (with detector cones) and orbits. The auroral electron precipitation oval is shown on the northern polar cap while ionospheric electron density contours cover the rest of the Earth.

---

(7) The Magnetospheric Specification Model (MSM), which generates time-dependent flux profiles of electron, H^+, and O^+ particle fluxes in the inner and middle magnetosphere,

(8) An empirical neutral atmosphere model (NRLMSISE-00),

(9) A new trapped proton science model and application (TPM-1) and related orbit integration application (TPM-1-APP),

(10) A TPM-1 application module, which calculates the omni-directional proton fluence along orbits,

(11) Updated and augmented graphical tools, e.g., the 1-D graphical tools to integrate plotted quantities and save the plot values to text files, and

(12) Six new detailed examples to enable the user to explore the new capabilities.

4.3. Spacecraft Charging and Charge Mitigation

4.3.1. NASA-Air Force Spacecraft Charging Analyzer Program (NASCAP-2K)

During the period of this report NASCAP-2K was used to design the electrostatic cleanliness guidelines for the AFRL C/NOFS satellite. In this instance, the concern was for very low levels of charging that could interfere with in situ electric field measurement. The analysis showed how thinner layers of indium tin oxide could be used to establish an equipotential surface over the solar cells. The thinner layer blocked less sunlight, reduced the solar cell count, and enabled a deployment approach that saved over $1M in AFRL funds   NASCAP-2K is currently being used to study the sheath and radiation efficiency of a large, high-voltage, Very Low Frequency (VLF) antenna in space. In this application the electron dynamics are treated as steady state while the ions are treated with time-stepped PIC. AFRL personnel have also been studying the physics of the VLF sheath independently of the NASCAP-2K contractual effort (Song et al., 2007). Figure 10 shows the NASCAP-2K user interface and examples of its output.

NASCAP-2K has also been used to study the anomaly encountered by the Special Sensor Ultraviolet Limb Imager (SSULI) on the operational DMSP satellite (Davis et al., 2006). The simulation showed that ions accelerated by the spacecraft potential have sufficient energy to penetrate electrostatic shields in the instrument, strike the detector, and thus contaminate the data.

4.3.2. Satellite Charge/Discharge Product (Char/D)

The following models and decision aids were incorporated in Char/D to specify or forecast the space environment and its effects on user-specified satellites: (1) the Hardy Aurora Model, (2) the CRRES Electron Radiation Belt Model, (3) the Korth MPA Data Model, (4) the SOPA/GOES Survey Model, (5) the Magnetospheric Specification Model, (6) the Deep Charging/Discharging Decision Aid, and (7) the Surface Charging Decision Aid (and its NASCAP-2K RealTime algorithm). Sample prototype graphical display software was also created and delivered with the basic software product. Note that while items (1), (2), and (4) represent existing environment models, all of the other items represent algorithms newly developed for this product. A complete description of the product is provided in the final report and ICD (Hilmer 2006a, 2006b).

The product is currently being integrated into the SSA Environmental Effects Fusion System (SEEFS), which is being built for Air Force Space Command. The spacecraft charging portion of SEEFS will specify and forecast space environment dangers to operational spacecraft. Potential benefits include preparing for space environmental consequences; enhancing anomaly resolution timelines; decreasing system downtime and improving satellite operations planning and execution (vehicle payload safe-hold procedures, payload tasking, etc.).
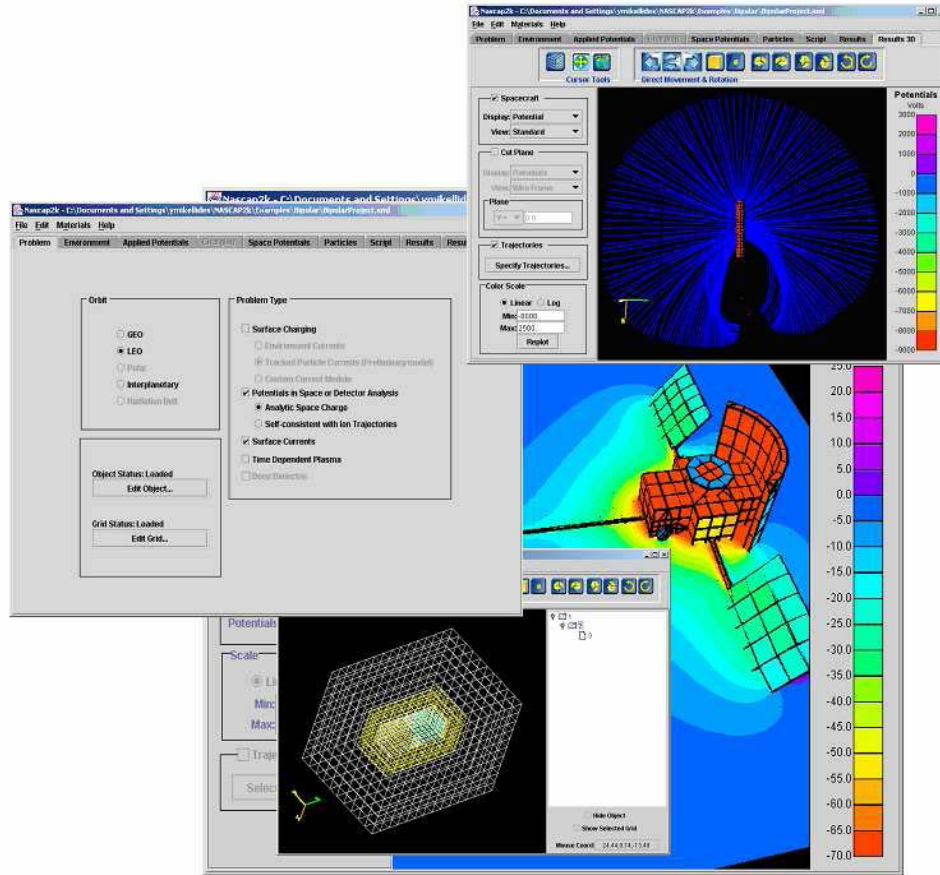
Figure 10. Views of the NASCAP-2K tabbed user interface, including main problem setup (center left), particle trajectories (upper right), and surface and space potentials.

_____

4.3.2.1. Hardy Aurora Model. The aurora module (also known as the Hardy Model) accesses the set of Air Force Statistical Auroral Models (AFSAM), a compilation of time averaged auroral ion and electron models (for details see Brautigam et al., 1991). These models were derived from measurements made by the SSJ/4 electrostatic analyzers flown on the DMSP-F6 and F7 satellites. The model output is used for display purposes only and includes integral electron and ion number flux, integral electron and ion energy flux, and electron and ion average energy.

4.3.2.2. CRRES Electron Radiation Belt Model. The CRRES Electron Radiation Belt Model accesses the CRRESELE model developed by Brautigam and Bell (1995). CRRESELE utilizes electron radiation belt measurements made by the High Energy Electron Fluxmeter (HEEF) flown on the Combined Release and Radiation Effects Satellite (CRRES). The model output is used for display purposes only and includes electron fluxes from ten energy channels covering 0.65 to 5.75 MeV.

4.3.2.3. Korth MPA Data Model. The Korth MPA Data Model was newly developed for this product. It is based on the work of Korth et al. (1999) and was constructed using 1996 MPA geosynchronous particle flux averages binned as a function

24

of the Kp index and local time. The 1996 mean particle data were provided to AFRL by Michelle Thomsen of LANL (private communication). Inputs are the Kp index and East Longitude (degrees) of a geosynchronous satellite. The model output is used for display purposes only and includes geosynchronous average electron and proton fluxes as well as the corresponding 10th and 90th percentile fluxes over the energies 2 eV to ~40 keV.

    4.3.2.4. SOPA/GOES Survey Model. The SOPA/GOES Survey Model is a newly developed application that uses LANL/SOPA and NOAA/GOES particle flux measurements to specify geosynchronous energetic electron fluxes at arbitrary longitudes. It has been demonstrated statistically by O'Brien et al. (2001) that if the electron belts are fairly quiet, then geosynchronous energetic electron fluxes at different longitudes are somewhat correlated. The model uses this concept to perform what is called a "peer-mapping" procedure, which can, for a given time interval, use average observed electron fluxes at one longitude to specify the same flux quantity at another arbitrary longitude. The SEEFS module described here was created by following pseudo-code of an algorithm provided by Paul O'Brien of the Aerospace Corporation (O'Brien, 2002). The SEEFS SOPA/GOES Survey Model algorithm performs the following basic tasks. For each time of interest, a chart is built containing 48 half-hour local time bins with all electron channel energies from the SOPA and GOES input data streams represented. Each local time bin is then populated via the peer-map procedure with flux values based on fluxes observed at all SOPA and GOES locations during the hour before that time. If multiple input sources are available, then the individual values mapped to a particular local time sector are averaged for use in the chart. Module output includes peer-mapped SOPA electron fluxes (7 channels spanning 315 keV to 6 MeV) and peer-mapped GOES >2 MeV electron fluxes appropriate to the geosynchronous satellite locations of interest. Note that SOPA/GOES Survey Model output is required as input for the geosynchronous part of the Deep Charging/Discharging Decision Aid described below.

    4.3.2.5. Magnetospheric Specification Model. The Magnetospheric Specification Model (MSM) uses environmental input parameters to produce time-dependent descriptions of electron and proton fluxes of energies 10 eV to 200 keV in the inner and middle magnetosphere (Freeman et al., 1993). The SEEFS module uses MSM Version 5.00 of 27 September 1994, the same version used in the validation study done by Hilmer and Ginet (2000). Extracting particle fluxes from MSM output results at arbitrary satellite locations is accomplished using the 20 October 1997 version of the MAP3D code of Hilmer et al. (1993). The 1997 update to MAP3D utilizes a code providing better three-dimensional interpretation of the magnetic neutral sheet location (Hilmer 1997). While the MSM module output can be displayed as part of an SSA tool, its real impact comes from generating the particle spectral inputs, i. e., electron and proton fluxes at 54 possible energies recorded at 1-minute intervals along each orbit, required by the Surface Charging Decision Aid described below. A sample of the MSM spectral output along a geosynchronous orbit is presented in Figure 11.
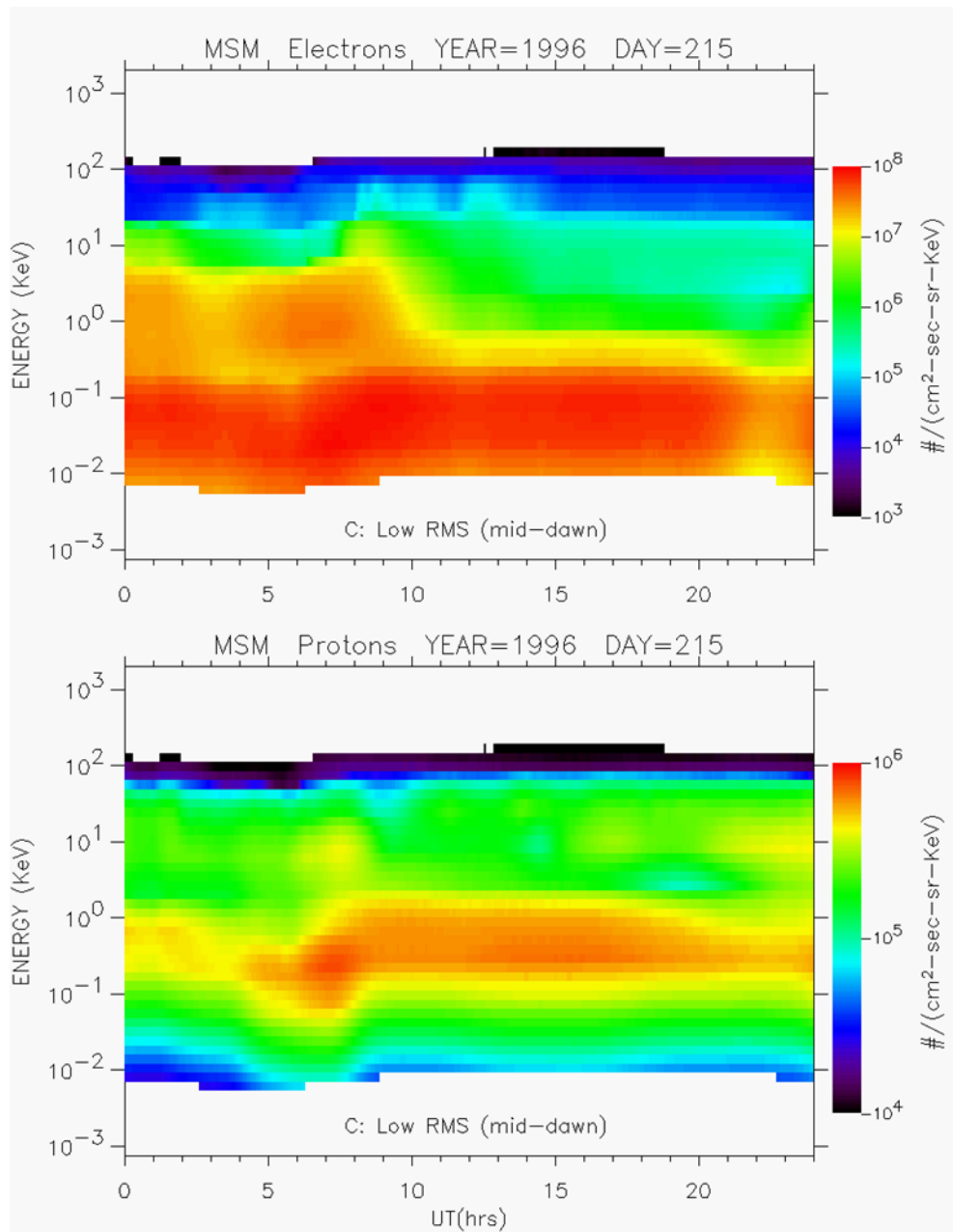
Figure 11. Electron and proton spectra specified by the MSM along the DSCS orbit path for day 215 of 1996 using input parameter set C.

4.3.2.6. Deep Charging/Discharging Decision Aid. The core of the SEEFS Deep Charging/Discharging Decision Aid is an empirical model that determines if electrostatic charge buildup is occurring in dielectrics inside spacecraft due to exposure to high flux/fluence levels of moderate-to-high energy electrons (>300 keV) and computes the probability of a resulting impulsive discharge. These electrons have sufficient energy to penetrate through the surface material of spacecraft and into dielectrics, hence the term "deep charging." Electrons with lower energies do not penetrate much beyond the

26

surface of a material and result in "surface charging." Surface charging is addressed in the Surface Charging Decision Aid described below.

One premise underlying the Deep Charging-Discharging Specification Product is that charging is the result of a non-equilibrium condition between charge accumulation and charge dissipation. Deep charge accumulation occurs whenever spacecraft material is exposed to moderate-to-high energy electrons, and the accumulation is assumed to be linearly proportional to amount of electrons encountered. This means most spacecraft undergo charge accumulation for a large fraction of each day, the specific fraction dependent on the spacecraft's orbit. Countering this charge accumulation is an intrinsic charge dissipation mechanism. The rate of charge dissipation depends on the specific spacecraft material and the specific spacecraft's design and fabrication. Charging occurs when the rate of charge accumulation exceeds the rate of the intrinsic charge dissipation. Electrostatic discharges do not accompany every period of charging. Discharges result from the formation of a new conduction path to a lower potential area due to either: dielectric breakdown caused by a very high space charge density resulting from charging by energetic electrons; or plasma formed by a micrometeoroid/orbital debris impact. The product is structured into two modules referred to here by the names *LEO/MEO* and *GEO/HEO*. First, the *LEO/MEO* module is used for spacecraft in low Earth orbit (LEO) or medium Earth orbit (MEO). In this case, the PBI values derived by the NOAA Space Environment Center from the NOAA/POES MEPED >300 keV electron flux measurements represent the charging condition and the resulting discharge condition is represented by the ground-level daily-averaged Climax Neutron Count Rate.

Second, the *GEO/HEO* module is used for spacecraft in geosynchronous Earth orbit (GEO) or highly elliptical orbit (HEO). In this case, the geomagnetic activity index Kp and the daily sum of 3-hour values, plus GOES >2 MeV electron data are used as inputs. The charging level is assumed to be proportional to the energetic electron flux experienced by the spacecraft. Also, the discharge likelihood is 72 hours prior to the time of interest. If GOES >2 MeV electron data are not available to run in nowcast mode, or if a forecast mode run is desired, then results from the Koons/Gorney Neural Net daily forecast model of >3 MeV electron flux at geosynchronous orbit (Koons and Gorney, 1991) are used as proxy input.

For both modules, user-specified charging thresholds are used to determine five basic output parameters: Internal (Deep) Charging Status, Internal (Deep) Discharge Status, Anomaly Probability Due to Internal Discharge, Probability Confidence Factor, and a Discharge Criterion. Due to a lack of significant detailed knowledge of spacecraft conditions, the output values assigned are based on a statistical picture of the measured environment and the occurrence rate of anomalies.

4.3.2.7. Surface Charging Decision Aid. The Surface Charging Decision Aid module provides estimates of spacecraft surface potentials resulting from exposure to electrons and protons (eV to 200 keV) within the plasma sheet of the magnetosphere. The resulting spacecraft chassis potential and minimum and maximum differential potentials can then be compared with system-specific thresholds provided by the user to estimate

system impacts. The required electron and proton flux specifications along spacecraft orbits are provided by the Magnetospheric Specification Model (MSM) module described above. The spacecraft surface charging algorithm described here, called "NASCAP-2K RealTime," uses the MSM environment specified on an orbit path along with a spacecraft geometry description to determine spacecraft surface potentials as a function of time. While an earlier investigation indicated that the MSM might serve as a suitable charged-particle source for spacecraft surface charging codes (see Hilmer et al., 2001), the MSM/ NASCAP-2K RealTime merger within the Surface Charging Decision Aid represents the first time this technique has been fully implemented.

The NASCAP-2K RealTime charging code developed for this product ingests the tabular spectra of MSM electrons and protons at 1-minute intervals and computes surface potentials on the spacecraft. A NASCAP-2K *Object Toolkit* description of spacecraft, including specification of rotating solar arrays, includes information about geometry and material types. At each time step, the code records the time, the maximum potential, the minimum potential, the conductor potentials, the confidence level, and the potentials on each surface. Confidence levels are basically quality flags indicating when inputs/outputs are within acceptable physical ranges. NASCAP-2K RealTime is a stand-alone Java application and uses a robust version of the Boundary Element Method (BEM) charging algorithms that were developed for NASCAP-2K and originally implemented in Java in the *SEE Interactive Spacecraft Charging Handbook* (http://see.msfc.nasa.gov/ee /model_charging.htm). The charging algorithms used are only appropriate to the low density plasma environments found at geostationary altitude. The algorithm used to determine the sun direction is also only appropriate to spacecraft at geostationary altitude, and eclipse status is also considered within the calculation. User-provided charging thresholds are included in the output files so spacecraft-specific effects can be tracked.

The sample MSM output shown in Figure 11 served as input to the surface charging decision aid run that produced the chassis potentials identified as case MSM C (yellow line) in the top panel of Figure 12.

While validation of the product output is currently underway, outputs along the geosynchronous orbit appear to be reasonable, for example, the cases denoted MSM C in Figure 12. Preliminary runs often result in the appearance of large positive chassis potentials, which correspond to gaps in MSM electrons during these same intervals. It is suspected that this type of charging does not normally occur because nature provides a steady population of very low-energy (< 10 eV) electrons that are not provided by the MSM. Typically, trapping of low energy electrons by positive surfaces is required to get the potentials of the sun-facing surfaces correct even if the electron flux is much larger than the ion flux. We conclude that large positive potentials like this are not expected at geosynchronous orbit and should be ignored when produced by the product. We emphasize again that the surface charging decision aid is really a prototype.
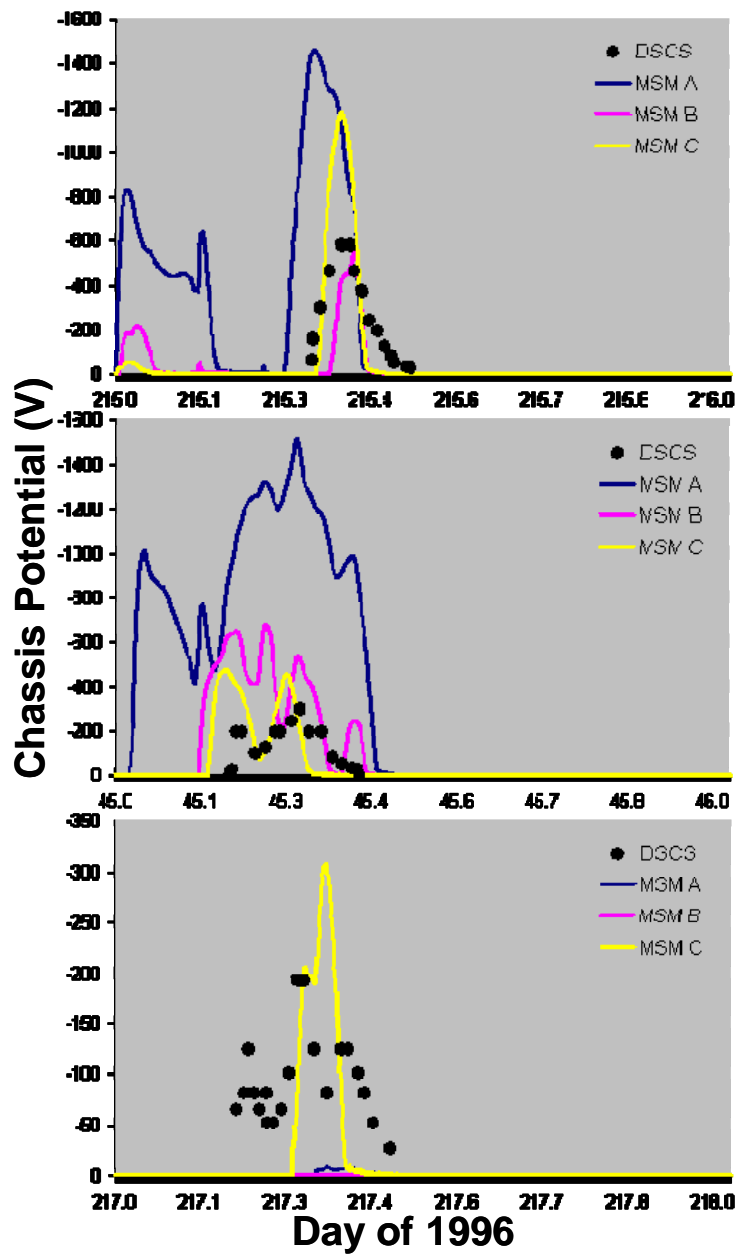
Figure 12. Chassis potentials measured on the geosynchronous spacecraft DSCS (black dots) and modeled potentials for three days in 1996. Potentials generated used spectra from the MSM (using input Sets A, B, and C) as input to the NASCAP-2K RealTime algorithm.

4.3.3. Spacecraft Charge Detection and Mitigation

Development of IProSEC has progressed steadily. The case for using a low-brightness cathode was made by Cooke and Geis (2002). They showed that a high

29

perveance can be obtained while using a low current to minimize space charge effects. (Perveance, $P = I V^{-3/2}$, is a measure of the current I delivered for a given voltage V from a cathode.) By accepting the low brightness of the cathode, a high total current can be achieved by increasing the total emission area. Geis et al. (2005) described the design and mechanism of these devices. Field emission occurs when electrons tunnel from a negatively biased cathode onto a positively doped substrate. If the substrate has no band gaps to absorb the electrons, they float on the surface until a gate or plasma ion creates a strong enough electric field to draw them off the surface. The initial tests of these devices, in which a physical gate was replaced with plasma ions, were reported by Wheelock et al. (2007) Successful operation in plasma was demonstrated, although operational limitations were observed when subjected to a high plasma flux. In that case enough current was emitted to melt the emission points and cause a sudden dropoff in emission.

IProSEC also contributes to another area of space technology that is peripheral to spacecraft charging, namely, the ElectroDynamic Tether (EDT). The EDT functions by exploiting the Lorentz force generated by the passage of current through a wire in a magnetic field, or the movement of a wire through a magnetic field. Studies and experiments have shown that the Lorentz force can be used as a means of in-space propulsion. The science of the EDT is closely related to spacecraft charging because they share the same physical concerns for current collection in the same space plasma. AFRL has contributed to the development of the EDT in two ways. One is through the development of IProSEC. The EDT must maintain current continuity by conducting through the ambient plasma, collecting electrons at one end and emitting them at the other. Emission requires a cathode, and of all the cathode technologies only IProSEC is passive and reversible. The other way in which AFRL has contributed to the EDT is by collaboration with an AFOSR-funded contract at MIT. This effort was aimed at understanding the anomalous enhancement in current collection observed by the TSS-1R tether mission (Cooke et al., 1995). A graduate student at MIT simulated the current enhancement of a positive wire in a flowing plasma as his doctoral research (Onishi, 2002). This work showed that the two-dimensional interaction of a wire displayed a similar enhancement (about a factor of 2) to that of the spherical (3-D) collector flown in TSS-1R.

Research into coupling of neutralizing electrons to electric propulsion plumes focused initially on the capability of PIC simulations to capture the effect. Wheelock et al. (2005) found that there was little coupling in the simulations, on the order of 10% of what would be expected. Adjusting the simulation parameters produced no discernable trend in coupling. Attempting to move beyond the physics captured in the simulations, Wheelock et al. (2006) examined the possibility of coulomb collisions and instabilities as coupling agents. Collisions alone were too weak to create the coupling action, even when a detailed account of collisions at larger angles was included. Collective instabilities, specifically the Buneman instability, showed similarities to the coupling that had been observed in simulation, but on a time scale that was comparatively an order of magnitude too large. Theoretical and simulation research on these effects is ongoing, in support of an experimental effort that began in late 2007.

5. CONCLUSIONS

The research effort has made significant progress in measuring energetic particles in the near-Earth space environment, developing and improving models of the environment and its effects on spacecraft, and developing techniques for mitigating electrostatic charge on spacecraft. Two Compact Environmental Anomaly Sensors were flown on the TSX-5 and DSP-21 satellites. TSX-5 operated for six years; DSP-21 continues to operate in its seventh year. We initiated development of a suite of space weather instruments that will be part of the Demonstration and Science Experiment (DSX) satellite, which is expected to be launched in 2010. When flown, these particle sensors will provide data vital to improving radiation belt and plasma models, particularly in the poorly quantified MEO orbit regime. Laboratory experiments were conducted to demonstrate the detection of RF emissions from high-velocity impacts. These experiments are part of an effort to develop a micrometeoroid impact detector for spacecraft. New and improved models of the space environment were incorporated into AF-GEOSpace, and Versions 2.0 and 2.1 were released to a wide range of users. Plans were formulated and work initiated on the development of new standard models of the radiation belts, to replace the existing AE-8 and AP-8 models. A Satellite Charge/Discharge Product (Char/D) was developed for the Technology Applications Division of the Space and Missile Systems Center at Peterson Air Force Base, Colo. Char/D combines observations and modeling of a wide range of electron energies in many magnetospheric regions to create tailored system-impact decision aids related to the specification and forecast of both surface and deep charging of satellites. NASCAP-2K was used to design the electrostatic cleanliness guidelines for the AFRL C/NOFS satellite. NASCAP-2K was also used to study an anomaly encountered by the SSULI instrument on the operational DMSP satellite; the simulation showed that ions accelerated by the spacecraft potential have sufficient energy to penetrate electrostatic shields in the instrument, strike the detector, and thus contaminate the data. A second-generation Charge Control System (CCS-II) was developed and will undergo testing in a laboratory vacuum chamber within the next year. Work on an alternative approach to neutralizing spacecraft charging, the Ion-Proportional Surface Emission Cathode (IProSEC), was initiated in collaboration with MIT Lincoln Laboratory.

These results will lead to improved spacecraft design, increased space situational awareness for space missions, and increased capability for space hazard mitigation. Future work will build on these results to produce improved versions of models and decision aids and increased capability for spacecraft protection. Continued miniaturization and expansion of instrument capabilities, for example, as envisioned for the Space Environment Distributed Anomaly Resolution System (SEDARS), will ensure cost-effective and comprehensive space situational awareness for DoD into the future.

REFERENCES

Brautigam, D. H., M. S. Gussenhoven, and D. A. Hardy (1991), A statistical study on the effects of IMF Bz and solar wind speed on auroral ion and electron precipitation, *J. Geophys. Res.*, **96**, 5525-5538.

Brautigam, D. H., and J. Bell (1995), CRRESELE Documentation, Tech. Rept. PL-TR-95-2128, Phillips Laboratory, Hanscom AFB, Mass., ADA 301770.

Brautigam, D. H., B. K. Dichter, K. P. Ray, W. R. Turnbull, D. Madden, A. Ling, E. Holeman, R. H. Redus, and S. Woolf (2001), Solar cycle variation of outer belt electron dose at low earth orbit, *IEEE Trans. Nucl. Sci.*, **48**: 2010–2015.

Brautigam, D. H., K. P. Ray, G. P. Ginet, and D. Madden (2004), Specification of the radiation belt slot region: Comparison of the NASA AE8 model with TSX5/CEASE data. *IEEE Trans. Nucl. Sci.*, **51**: 3375–3380.

Compact Environmental Anomaly Sensor II, Advanced Concept Technology Demonstration, Final Report, Space Warfare Center, Schriever AFB, Colo., 2003 (signed 16 Jun 2004).

Cooke, D. L., and M. W. Geis (2002), Introducing the passive anode surface emission cathode, 38th AIAA/ASME/SAE/ASEE Joint Propulsion Conference and Exhibit, Indianapolis, Ind., AIAA-2002-4049.

Davis, V. A., M. J. Mandell, B. M. Gardner, I. G. Mikellides, L. F. Neergaard, D. L. Cooke, and J. Minor (2004), Validation of NASCAP-2K Spacecraft-Environment Interactions Calculations, *Proc. 8th Spacecraft Charging Technology Conference*, Oct 2003, Huntsville, Ala., *NASA/CP-2004-213091*.

Davis, V. A., M. J. Mandell, F. J. Rich, and D. L. Cooke (2006), Reverse trajectory approach to computing ionospheric currents to the Special Sensor Ultraviolet Limb Imager on DMSP, *IEEE Trans. Plasma Sci.*, **34**, No. 5, 2062–2070.

Dichter, B. K., J. O. McGarity, M. R. Oberhardt, V. T. Jordanov, D. J. Sperry, A. C. Huber, J. A. Pantazis, E. G. Mullen, G. P. Ginet and M. S. Gussenhoven (1998), Compact Environmental Anomaly Sensor (CEASE): A novel spacecraft instrument for *in situ* measurement of environmental conditions, *IEEE Trans. Nucl. Sci.*, **45**, No. 6: 2758.

Dichter, B. K., W. R. Turnbull, D. H. Brautigam, K. P. Ray, and R. H. Redus (2001), Initial on-orbit results from the Compact Environmental Anomaly Sensor (CEASE), *IEEE Trans. Nucl. Sci.*, **48**: 2022–2028.

Dichter, B. K., J. O. McGarity, M. Golightly, D. Brautigam and S. Woolf (2006), Calibration Report for the Particle Telescope on the Compact Environment Anomaly Sensor (CEASE), AFRL-VS-HA-TR-2006-1098, Air Force Research Laboratory, Hanscom AFB, Mass.

Freeman Jr., J. W., R. A. Wolf, R. W. Spiro, G.-H. Voigt, B. A. Hausman, B. A. Bales, R. V. Hilmer, A. Nagai, and R. Lambour (1993), Magnetospheric Specification Model: Development Code and Documentation, Final report for USAF contract F19628-90-K-0012, Rice University.

Geis, M. W., S. Deneault, K. E. Krohn, M. Marchant, T. M. Lyszczarz, and D. L. Cooke (2005), Field emission at 10 V cm^{-1} with surface emission cathodes on negative-electron-affinity insulators, *Appl. Phys. Lett.*, **87**, 192115.

Ginet, G. P., B. K. Dichter, D. Madden, and D. H. Brautigam (2007a), Energetic proton maps for the South Atlantic Anomaly, Radiation Effects Data Workshop, 2007 IEEE NSREC, 23–27 Jul 2007.

Ginet, G. P., B. K. Dichter., D. H. Brautigam and D. Madden (2007b), Proton flux anisotropy in low earth orbit, *IEEE Trans. Nucl. Sci.*, **54**: 1975–1980.

Golightly, M., and C. Knorring (2005), Empirical determination of a detector's geometric factor through intercomparison of coincident measurements on two different spacecraft, *EOS, Trans. AGU*, **86** (52), Fall Meeting Supp., Abstract SM41A-1171.

Hilmer, R. V. (1997), A magnetospheric neutral sheet-oriented coordinate system for MSM and MSFM applications, Tech. Rept., PL-TR-97-2133, Phillips Laboratory, Air Force Materiel Command, ADA 338067.

Hilmer, R. V., ed. (1999), AF-GEOSpace User's Manual, Version 1.4 and Version 1.4P, Tech. Rept. AFRL-VS-TR-1999-1551, Air Force Research Laboratory, Hanscom AFB, Mass., ADA389056.

Hilmer, R. V. (2002), AF-GEOSpace User's Manual, Version 2.0 and Version 2.0P, Air Force Research Laboratory, Hanscom AFB, Mass.

Hilmer, R. V., (2006a), Report on the SEEFS Satellite Charging/Discharging Product, SEEFS Satellite Char/D Product Version 1.0, submitted to Technology Application Division (SMC/WXT), Peterson AFB, Colo., 20 Jan 2006.

Hilmer, R. V. (2006b), Interface Control Document for The SEEFS Satellite Charging/Discharging Product, SEEFS Satellite Char/D Product Version 1.0, submitted to Technology Application Division (SMC/WXT), Peterson AFB, Colo., 15 Jun 2005 (updated 20 Jan 2006).

Hilmer, R. V. (2006c), AF-GEOSpace User's Manual, Version 2.1 and Version 2.1P, Air Force Research Laboratory, Hanscom AFB, Mass. (http://www.kirtland.af.mil/shared/media/document/AFD-070402-067.pdf).

Hilmer, R. V., and G. P. Ginet (2000), A magnetospheric specification model validation study: Geosynchronous electrons, *J. Atmos. & Solar-Terr. Phys.,* **62**, 1275.

Hilmer, R. V., R. A. Wolf, and B. A. Hausman (1993), Mapping *Magnetospheric Specification Model* results to arbitrary positions in the 3-D magnetosphere: Development of FORTRAN application codes MAP3D and FLUX3D, Final report for Hughes STX Corp. subcontract No. 93-F04-I1902, Rice University.

Hilmer. R. V., G. P. Ginet, D. L. Cooke, and I. Katz (2001), Space weather forecasting: under the hood of the Magnetospheric Specification Model, Proc. *7th Spacecraft Charging Technology Conference*, April 2001, ESTEC, The Netherlands. ESA SP-476, p. 235.

Hilmer, R. V., G. P. Ginet, T. Hall, E. Holeman, and M. F. Tautz (2004), AF-GEOSpace 2.0, *Proc. 8th Spacecraft Charging Technology Conf.*, Huntsville AL, Oct. 20-24, 2003, J. L. Minor, Compiler (AFRL-VS-HA-TR-2004-1010, Air Force Research Laboratory, Hanscom AFB, Mass.).

Katz, I., P. R. Stannard, L. Gedeon, J. C. Roche, A. G. Rubin, and M. F. Tautz (1983), NASCAP Simulations of Spacecraft Charging of the SCATHA Satellite, *Spacecraft/Plasma Interactions and their Influence on Field and Particle Measurements, ESA SP-198*, 109.

Koons, H. C., and D. J. Gorney (1991), A neural network model of the relativistic electron flux at geosynchronous orbit, *J. Geophys. Res.*, **96**, 5549.

Korth, H., M. F. Thomsen, J. E. Borovsky, and D. J. McComas (1999), Plasma sheet access to geosynchronous orbit, *J. Geophys. Res.,* **104**, 25047-25061.

MacNeice, P., K. M. Olson, C. Mobarry, R. deFainchtein, and C. Packer (2000), PARAMESH: A parallel adaptive mesh refinement community toolkit, *Computer Physics Communications*, **126**, 330-354.

Maki, K., E. Soma, T. Takano, A. Fujiwara, A. Yamor (2005), Dependence of microwave emissions from hypervelocity impacts on the target material, *J. Appl. Phys.*, **97**: 104911.

Mandell, M. J., V. A. Davis, B. M. Gardner, I. G. Mikellides, D. L. Cooke, and J. Minor (2004), NASCAP-2K – An Overview, Proc. *8th Spacecraft Charging Technology Conference*, Oct. 2003, Huntsville, Ala., *NASA/CP-2004-213091*.

Mandell, M. J., D. L. Cooke, V. A. Davis, G. A. Jongeward, and B. M. Gardner, R. A. Hilmer, K. P. Ray, S. T. Lai, and L. H. Krause (2005), Modeling the charging of geosynchronous and interplanetary spacecraft using NASCAP-2K (34th COSPAR, Houston, Tex., *Advances in Space Research*, **36**, No. 12, 2511–2515.

Mandell, M. J., V. A. Davis, D. L. Cooke, A. T. Wheelock, and C. J. Roth (2006), NASCAP-2K spacecraft charging code overview, *IEEE Trans. Plasma Sci.*, **34**, No. 5, 2084–2093.

Metcalf, J., J. Albert, D. Brautigam, G. Ginet, M. Golightly, C. Knorring, S. Lai, E. Murad, and S. Young (2007), Space Particle Hazard Measurement and Modeling, AFRL-RV-HA-TR-2007-1146, Air Force Research Laboratory, Hanscom AFB, Mass.

Mullen, E. G., and K. P. Ray (1994), Microelectronics effects as seen on CRRES, *Adv. Space Res.*, **14**, No. 10: 797–807.

Mullen, E. G., K. P. Ray, R. Koga, E. G. Holeman, and D. E. Delorey (1995), SEU results form the Advanced Photovoltaic and Electronics Experiments (APEX) satellite, *IEEE Trans. Nucl. Sci.*, **42**: 1988–1994.

O'Brien, T. P., D. Sornette, and R. L. McPherron (2001), Statistical asynchronous regression: Determining the relationship between two quantities that are not measured simultaneously, *J. Geophys. Res.,* **106**, 13247-13259.

O'Brien, T. P. (2002), SOPA Survey Model Description (Document Version 4.1), private communication, 16 Aug 2002.

Onishi, T. (2002), *Numerical Study of Current Collection by an Orbiting Bare Tether*, Ph. D. Thesis, Mass. Inst. of Tech. (dspace.mit.edu).

Redus, R. H. (2003), Compact Environmental Anomaly Sensor Instrument Description, Report #SRA-0002-B0, Amptek, Inc., Bedford, Mass.

Song, P., B. W. Reinisch, V. Paznukhov, G. Sales, D. Cooke, J.-N. Tu, X. Huang, K. Bibl, and I. Galkin (2007), High-voltage antenna-plasma interaction in whistler wave transmission: plasma sheath effects, *J. Geophys. Res.*, **112**, A03205, doi:10.1029/2006JA011683.

Spanjers, G., J. Winter, D. Cohen, A. Adler, J. Guarnieri, M. Tolliver, G. P. Ginet, B. K. Dichter, and J. Summers (2006), The AFRL Demonstration and Science Experiments (DSX) for DoD Space Capability in the MEO, IEEE Aerospace Conference, 4-11 Mar 2006: 1–10.

Stannard, P. R., I. Katz, L. Gedeon, J. C. Roche, A. G. Rubin, and M. F. Tautz (1982), Validation of the NASCAP model using spaceflight data, *American Institute of Aeronautics and Astronautics, AIAA 82-0269*.

Starks, M. J., D. L. Cooke, B. K. Dichter, L. C. Chhabildas, W. D. Reinhart, T. F. Thornhill III (2006), Seeking radio emissions from hypervelocity micrometeoroid impacts: Early experimental results from the ground, *Intl. J. Impact Eng.*, **33**: 781.

Wheelock, A. T., D. L. Cooke, and N. A. Gatsonis (2005), Computational analysis of current coupling of ion beam-neutralizer interactions, 41st Joint Propulsion Conf., Tucson, Ariz., AIAA 2005-3692.

Wheelock, A. T., D. L. Cooke, N. A. Gatsonis (2006), Electron-ion beam coupling through collective interactions, 42nd AIAA/ASME/SAE/ASEE Joint Propulsion Conference and Exhibit, Sacramento, Calif., AIAA-06-5024.

Wheelock, A. T., D. L. Cooke, and M. W. Geis (2007), Initial plasma tests of the IProSEC cathode device, 10th Spacecraft Charging Technology Conf., Biarritz, France.

Appendix A

Modules in AF-GEOSpace Version 2.1

APEXRAD: The Advanced Photovoltaic and Electronics Experiments (APEX) space radiation dose model specifies the location and intensity of the radiation dose rate behind four different thicknesses of aluminum shielding for five geomagnetic activity levels. It covers the low Earth orbit (LEO) altitude region (360-2400 km) and was developed to supplement the CRRESRAD model (see below), which has limited resolution in the LEO regime.

APEXRAD-APP: The Advanced Photovoltaic and Electronics Experiments (APEX) radiation dose application calculates expected accumulated yearly dose along a user-specified orbit for four thicknesses of aluminum shielding during four levels of magnetic activity. Best for orbits with apogees less than 2500 km (see the CRRESRAD-APP for higher altitudes).

AURORA: The auroral precipitation model specifies the location and intensity of electron number and energy flux, ion number and energy flux, Pederson and Hall conductivities, and the equatorward boundary at 110 km altitude. This module also provides the capability to map flux, conductivity, and equatorial boundary values up magnetic field lines into the three-dimensional magnetospheric grid.

BFIELD-APP: The B-Field application allows the generation of data sets representing the magnetic field in the near-Earth space environment. A variety of internal (dipole, IGRF) and external field models are used to generate gridded data set, field lines, and flux tubes.

BFOOTPRINT-APP: This application traces geomagnetic field-lines from single user-specified points (defined in either geographic or magnetic coordinates) or multiple points along a satellite orbital track. The resulting field-lines, orbital track, and list of footprint locations on the Earth's surface can be viewed.

COORD_TRANSFORM: This worksheet performs coordinate transformations on point locations using different coordinate systems (GEOC, GSM, SM, GEI) and coordinate geometries (Cartesian, Cylindrical, Spherical) at a given Year, Day, and UT.

CHIME: The CRRES/SPACERAD Heavy Ion Model of the Environment (CHIME) specifies the location and intensity of galactic cosmic rays and/or solar energetic particle fluxes and/or anomalous cosmic ray fluxes.

CRRESELE: The Combined Radiation and Release Effects Satellite (CRRES) electron flux model specifies the location and intensity of electron omni-directional flux over the energy range 0.5-6.6 MeV for a range of geomagnetic activity levels.

CRRESELE-APP: The CRRESELE application traces user-specified orbits through the CRRES electron flux models to provide an estimate of electron fluence received by the satellite under a wide range of magnetospheric conditions.

CRRESPRO: The Combined Radiation and Release Effects Satellite (CRRES) proton flux model specifies the location and intensity of proton omni-directional flux over the energy range 1-100 MeV for quiet, average, or active geophysical conditions.

CRRESPRO-APP: The CRRESPRO application uses the CRRES proton flux model to calculate omni-directional proton fluence (integral and differential) over the range 1 to 100 MeV for user specified orbits and quiet, active, or average geophysical activity levels.

CRRESRAD: The Combined Radiation and Release Effects Satellite (CRRES) space radiation dose model specifies the location and intensity of the radiation dose rate behind four different thicknesses of aluminum shielding for active or quiet geophysical activity levels.

CRRESRAD-APP: The CRRESRAD application uses the CRRES space radiation dose model to calculate expected satellite dose accumulation behind four different thicknesses of aluminum shielding for user-specified orbits for active or quiet geophysical activity levels.

CUTOFF: This module accesses the Geomagnetic Vertical Cutoff Rigidity Interpolation Model to provide cutoff rigidity values for solar protons and cosmic rays, as a function of the geomagnetic activity index Kp, for any altitude from in the Earth's atmosphere ($\geq$ 20 km) to beyond geosynchronous orbit

DMSP: The DMSP data module displays the particle spectra and integrated precipitating flux from the DMSP SSJ4/5 particle sensors, which are used to determine auroral precipitation boundaries.

EPHEMERIS: This module enables the display of spacecraft orbits and on-board detector data that are read from user-generated satellite ephemeris/data files.

IONSCINT: The High Fidelity Ionospheric Scintillation Simulation Algorithm (IONSCINT) model provides realistic scenarios of disruptions in trans-ionospheric radio wave communications with spacecraft due to equatorial scintillation. IONSCINT addresses only intensity (or amplitude) scintillation of 244 MHz signals from geosynchronous satellites.

ISPM: The Interplanetary Shock Propagation Model predicts the transit time of interplanetary shocks from the Sun to the Earth and the shock strength upon arrival.

LET-APP: The LET application calculates the linear energy transfer (LET) spectrum and its associated single event upset (SEU) rate in a microelectronic device resulting from the penetration of energetic space particles. Effects from both cosmic rays and the trapped protons are estimated by using the CHIME and CRRESPRO models as inputs.

METEOR IMPACT: The Meteor Impact Map Model calculates the hourly meteor impact rate or damage rate for a given cross section, pit depth, and material type on a user-specified surface area at positions outside of the Earth's atmosphere. A yearly shower database is used to determine the active showers, their intensity, direction of travel, and mass distribution characteristics.

METEOR IMPACT-APP: The Meteor Impact Map Model application calculates meteor flux or damage rates for given cross section, pit depth, and material type as a function of time along a user-specified orbit. Cumulative probabilities for flux and damage rates are also determined.

METEOR SKY MAP: The Meteor Sky Map module calculates the number of visible meteors from active meteor showers (and any user-specified storms) at the specified date, over a grid of ground-level positions covering the entire globe.

MSM: The Magnetospheric Specification Model (MSM) module generates time-dependent electron, H^+, and O^+ particle fluxes in the inner and middle magnetosphere in the energy range 100 eV to 200 keV.

NASAELE: The NASA AE-8 radiation belt models are used to compute the intensity and location of differential omni-directional electron flux for ten energy intervals between 0.5 and 6.6 MeV.

NASAELE-APP: The NASAELE application traces a user-specified orbit through the NASA AE-8 trapped electron model to provide an estimate of electron fluence received by the satellite under a wide range of magnetospheric conditions.

NASAPRO: The NASA AP-8 radiation belt models are used to compute the intensity and location of differential omni-directional proton flux for 22 energy intervals between 1 and 100 MeV.

NASAPRO-APP: The NASAPRO application calculates proton omni-directional fluence (differential and integral) over the energy range 1.5-81.3 MeV for user specified orbits and quiet or active geophysical conditions using the NASA AP-8 trapped proton model.

NRLMSISE-00: The NRLMSISE-00 empirical model computes atmospheric number densities of He, O, N_2, O_2, Ar, H, and N, plus total mass density and temperature. Anomalous oxygen number density, i.e., hot atomic oxygen (O_h) or atomic oxygen ions (O^+) present at high altitudes (>500 km), and exospheric temperature are also calculated.

PARAMESH: This data visualization module allows the user to load MHD science code simulation run results (produced externally to AF-GEOSpace) that are stored in large-scale structured grids using the Parallel Adaptive Mesh Refinement (PARAMESH) file format (MacNeice et al., 2000).

PIM: The Parameterized Ionospheric Model (PIM) generates global electron number density as well as maps of total electron content (TEC), Height of E and F2 peaks (HE, HF2), and plasma frequencies at the E and F2 peaks (FoE, FoF2) as a function of a variety of geophysical activity indices.

PPS: The Proton Prediction System (PPS) provides forecasts of the intensity and duration of solar proton events.

RAYTRACE-APP: The ray tracing application calculates the behavior of MHz rays in an ionosphere specified by a Parameterized Ionosphere Model (PIM) data set.

SATEL-APP: The satellite application calculates orbital trajectories for satellites from a variety of user specified orbital element input sets.

SEEMAPS: The Single Event Effects Maps (SEEMAPS) module uses normalized flux and dose data for protons with energy > 50 MeV from the APEX and CRRES satellites to produce contour maps of relative probabilities of experiencing Single Event Effects (SEEs) in the Earth's inner radiation belts.

STOA: The Shock Time-of-Arrival (STOA) model predicts the transit time of interplanetary shocks from the Sun to the Earth. STOA is a predecessor of ISPM.

TPM-1: The Trapped Proton Model (TPM-1) provides a solar-cycle dependent low-altitude extension to the CRRESPRO trapped energetic proton model.

TPM-1-APP: The TPM-1 application uses the TPM-1 proton flux model to calculate omni-directional proton fluence (integral and differential) over the range 1 to 100 MeV.

WBMOD: The WideBand Model (WBMOD) is an RF ionospheric scintillation model specifying S4, SI, and other scintillation parameters between ground stations and satellites above 100 km altitude. An associated application gives a 24 hour WBMOD climatology prediction of the dB fade levels due to ionospheric scintillation effects for specific ground-to-satellite communication links.

Abbreviations and Acronyms

ACE	Advanced Composition Explorer
ACTD	Advanced Concept Technology Demonstration
AFRL	Air Force Research Laboratory
AFSAM	Air Force Statistical Auroral Models
AFSPC	Air Force Space Command
AFWA	Air Force Weather Agency
BEM	Boundary element method
CAD	Computed aided design
CCD	Charge-coupled device
CCS	Charge Control System
CEASE	Compact Environmental Anomaly Sensor
CIV	Critical ionization velocity
CONOPS	Concept of Operations
CRRES	Combined Release and Radiation Effects Satellite
DCTB	Defensive Counterspace Test Bed
DMSP	Defense Meteorological Satellite Program
DSCS	Defense Satellite Communications System
DSP-21	Defense Support Program 21 satellite
DSX	Demonstrations and Science Experiment
EDT	Electrodynamic Tether
EMIC	Electromagnetic ion cyclotron
EPS	Energetic Particle Sensor
ESA	Electrostatic analyzer
ESP	Energetic Spectrometer for Particles
FLC	Field line curvature
FOG	Fiber-optic gyroscope (on TSX-5)
GEO	Geosynchronous Earth orbit
GOES	Geostationary Operational Environmental Satellite
GTO	Geosynchronous transfer orbit
HEO	Highly elliptical orbit
HEPS	High Energy Proton Spectrometer
HF	High frequency
HiLET A	High Linear Energy Transfer-A (0.8–3.0 MeV)
HiLET B	High Linear Energy Transfer-B (3.0–10.0 MeV)
HIPS	High Energy Imaging Particle Spectrometer
HR	Hazard register (on CEASE)
IProSEC	Ion-Proportional Surface Emission Cathode
IR	Infrared
LANL	Los Alamos National Laboratory
LEESA	Low Energy Electrostatic Analyzer
LEO	Low Earth orbit
LIPS	Low Energy Imaging Particle Spectrometer
LoLET	Low Linear Energy Transfer (0.05–0.85 MeV)
MEO	Medium Earth orbit

MEPED	Medium Energy Proton/Electron Detector
MHD	Magneto-hydrodynamic
MPA	Magnetospheric Plasma Analyzer
NASA	National Aeronautics and Space Administration
NASCAP-2K	NASA-Air Force Spacecraft Charging Analyzer Program
NOAA	National Oceanic and Atmospheric Administration
MIT	Massachusetts Institute of Technology
MSM	Magnetospheric Specification Model
PBI	POES Belt Index
PIC	Particle-in-cell
POES	Polar Operational Environmental Satellite
QLP	Quadrature Langmuir probe
RFI	Radio frequency interference
SCTC	Spacecraft Charging Technology Conference
SDTW	Space Development and Test Wing (formerly STP)
SEE	Single event effect
SEEFS	SSA Environmental Effects Fusion System
SEDARS	Space Environment Distributed Anomaly Resolution System
SEP	Solar energetic proton
SEU	Single event upset
SNL	Sandia National Laboratories
SOPA	Synchronous Orbit Particle Analyzer
SPE	Solar proton event
SSA	Space Situational Awareness
SSULI	Special Sensor Ultraviolet Limb Imager
STP	Space Test Program
STRV-1c	Space Technology Research Vehicle 1c satellite
TSX-5	Tri-Service Experiment 5 satellite
VLF	Very low frequency
WF	Warning flag (on CEASE)